NACA RM L57A30

NACA

RESEARCH MEMORANDUM

EXPERIMENTAL DETERMINATION AT SUBSONIC SPEEDS OF THE OSCILLATORY AND STATIC LATERAL STABILITY DERIVATIVES OF A SERIES OF DELTA WINGS WITH LEADING-EDGE SWEEP FROM 30° TO 86.5°

By William Letko

Langley Aeronautical Laboratory
Langley Field, Va.

NATIONAL ADVISORY COMMITTEE
FOR AERONAUTICS

WASHINGTON

April 12, 1957
Declassified April 15, 1958

NATIONAL ADVISORY COMMITTEE FOR AERONAUTICS

RESEARCH MEMORANDUM

EXPERIMENTAL DETERMINATION AT SUBSONIC SPEEDS OF THE OSCILLATORY AND STATIC LATERAL STABILITY DERIVATIVES OF A SERIES OF DELTA WINGS WITH LEADING-EDGE SWEEP FROM 30° TO 86.5°

By William Letko

SUMMARY

The static lateral stability of six delta wings was determined at subsonic speeds and, in addition, two of the wings with 82.5° and 75° sweep of the leading edge were oscillated in yaw about the 50-percent point of the root chord in order to determine the effects of frequency and amplitude on the combination lateral stability derivatives resulting from this motion.

The results of the oscillation tests showed that large changes in the derivatives occurred with changes of frequency and amplitude at the high angles of attack for the 82.5° and 75° delta wings. For the reduced frequency parameter $\frac{\omega b}{2V} = 0.066$ the largest changes in the derivatives with amplitude generally occurred at low values of amplitude. Comparison of the variation with angle of attack of the oscillatory derivatives obtained with the 82.5° and 75° wings with those of a 60° wing of another investigation showed that large differences in the oscillatory derivatives are generally obtained at the higher angles of attack and that the values of the combination oscillatory derivatives $C_{n_{\beta,\omega}} + k^2 C_{n_{\dot{r},\omega}}$ and $C_{l_{r,\omega}} - C_{l_{\dot{\beta},\omega}}$ for the 82.5° wing are very large and of opposite sign to those of the other wings. This comparison was made for one frequency and amplitude of oscillation. The results of the static tests showed that the static lateral stability derivatives followed trends which were similar to those of other investigations.

INTRODUCTION

Reference 1 has pointed out the necessity of including the acceleration derivatives $C_{n_{\dot{\beta}}}$ and $C_{l_{\dot{\beta}}}$ as determined from oscillation tests

in calculations of dynamic lateral stability. This is especially true at the high angles of attack since references 2 and 3 show that rather large values of the acceleration derivatives may occur for certain configurations under these conditions. Since a 60° delta wing showed high values of oscillatory yawing derivatives at high angles of attack (refs. 2 and 3), information concerning the oscillatory yawing derivatives of narrow delta wings, which might be used in missile configurations, was thought to be of interest. The present investigation was undertaken, therefore, to provide some information regarding the effects of frequency and amplitude on narrow delta wings oscillating in yaw at angles of attack from 0° to the angle of maximum lift.

The present investigation consisted of determining the effects of a systematic variation of frequency and amplitude of oscillation on the oscillatory derivatives of 82.5° and 75° delta wings. Static stability for these and for 86.5°, 60°, 45°, and 30° delta wings was also determined. Oscillatory derivatives for a 60° delta wing from reference 3 are also presented for comparison purposes. The oscillatory derivatives from reference 3 and those obtained in the present investigation were obtained by a forced oscillation technique; the motion was a combination of yawing and sideslipping and provided the combination derivatives $C_{n_{r,\omega}} - C_{n_{\dot{\beta},\omega}}$, $C_{l_{r,\omega}} - C_{l_{\dot{\beta},\omega}}$, $C_{n_{\beta,\omega}} + k^2 C_{n_{\dot{r},\omega}}$, and $C_{l_{\beta,\omega}} + k^2 C_{l_{\dot{r},\omega}}$ where k is the reduced frequency parameter $\omega b/2V$.

COEFFICIENTS AND SYMBOLS

All stability parameters and coefficients are referred to the stability system of axes originating at a center-of-gravity position of 50 percent of the root chord and in the chord plane of the wings investigated. (See fig. 1.)

C_L lift coefficient, F_L/qS

C_D' drag coefficient (approximate), F_D'/qS

C_Y lateral force coefficient, F_Y/qS

C_l rolling-moment coefficient, M_X/qSb

C_m pitching-moment coefficient, M_Y/qSb

C_n yawing-moment coefficient, M_Z/qSb

F_L lift

$F_{D'}$ drag (approximate)

F_Y lateral force

M_X rolling moment

M_Y pitching moment

M_Z yawing moment

α angle of attack, deg

b span, ft

β angle of sideslip, radians or deg

$\dot{\beta} = \frac{\partial \beta}{\partial t}$

β_o amplitude of sideslip, deg

$\bar{c}$ mean aerodynamic chord, ft

k reduced frequency parameter, $\frac{\omega b}{2V}$

ω circular frequency of oscillation, radians/sec

ψ angle of yaw, radians or deg

$\dot{\psi} = \frac{\partial \psi}{\partial t} = r$

ψ_o amplitude of yaw, deg

$\dot{r} = \frac{\partial r}{\partial t}$

q dynamic pressure, $\frac{1}{2}\rho V^2$, lb/sq ft

ρ mass density of air, slugs/cu ft

S wing area, sq ft

t time, sec

V free-stream velocity, ft/sec

$$C_{Y_\beta} = \frac{\partial C_Y}{\partial \beta}$$

$$C_{n_\beta} = \frac{\partial C_n}{\partial \beta}$$

$$C_{n_{\dot{\beta}}} = \frac{\partial C_n}{\partial \left(\frac{\dot{\beta} b}{2V}\right)}$$

$$C_{n_r} = \frac{\partial C_n}{\partial \left(\frac{rb}{2V}\right)}$$

$$C_{n_{\dot{r}}} = \frac{\partial C_n}{\partial \left(\frac{\dot{r} b^2}{4V^2}\right)}$$

$$C_{l_\beta} = \frac{\partial C_l}{\partial \beta}$$

$$C_{l_{\dot{\beta}}} = \frac{\partial C_l}{\partial \left(\frac{\dot{\beta} b}{2V}\right)}$$

$$C_{l_r} = \frac{\partial C_l}{\partial \left(\frac{rb}{2V}\right)}$$

$$C_{l_{\dot{r}}} = \frac{\partial C_l}{\partial \left(\frac{\dot{r} b^2}{4V^2}\right)}$$

All derivatives are nondimensional in this paper. The symbol ω following the subscript of a derivative denotes the oscillatory derivative.

APPARATUS AND MODELS

Oscillation Apparatus

The equipment used to oscillate the models consisted of a motor-driven flywheel, connecting rod, crank arm, and model support strut shown schematically in figure 2 and photographically in figures 3 and 4.

The connecting rod was pinned to an eccentric center on the flywheel and transmitted a sinusoidal yawing motion to the support strut by means of the crank arm. The models were fastened to the support strut at their assumed centers of gravity and the oscillation was forced about the vertical wind, or stability, axes of the models. The apparatus was driven by a one-horsepower direct-current motor through a geared speed reducer. The frequency of oscillation was varied by changing the voltage supplied to the motor, and the amplitude of oscillation was varied by adjusting the throw of the eccentric on the flywheel.

Models

Six delta wings were tested in the present investigation. The wings had leading-edge sweepback of 86.5°, 82.5°, 75°, 60°, 45°, and 30° and had aspect ratios 0.25, 0.53, 1.07, 2.31, 4.0, and 6.93, respectively. A sketch giving the geometric characteristics of the wings is presented as figure 5, and the characteristics are also listed in table I. Each of the wings was essentially a flat-plate airfoil made of 3/4-inch plywood with a circular leading edge and a beveled trailing edge. The trailing edges of all the wings were beveled to provide a trailing-edge angle of about 10° that was constant across the span.

Recording of Data

The recording of data was accomplished by means of the equipment described completely in the appendix of reference 4. Briefly, the rolling and yawing moments acting on the model during oscillation were measured by means of resistance-type strain gages, mounted on the oscillating strut, to which the model was attached. The moments were modified by a sine-cosine resolver driven by the oscillating mechanism so that the output signals of the strain gages were proportional to the in-phase and out-of-phase components of the strain-gage signals. These signals were read from a highly damped direct-current meter, and the aerodynamic coefficients were obtained by multiplying the meter readings by the appropriate constants, one of which was the system calibration constant.

TESTS

All tests were conducted in the 6- by 6-foot test section of the Langley stability tunnel at a dynamic pressure of 24.9 lb/sq ft which corresponds to a Mach number of 0.13. The Reynolds number based on the mean aerodynamic chord of the wings varied from approximately 8×10^5 for the 30° delta wing to 2.5×10^6 for the 86.5° delta wing. Static

lateral stability derivatives of all the wings were obtained from tests at angles of attack from -4° up to and beyond the maximum lift of each wing at angles of sideslip of ±5°.

The oscillation tests at an amplitude of 6° ($\pm\psi_o$) were conducted through the angle-of-attack range (in 10° increments) at frequencies of oscillation of 0.99, 1.81, 2.53, 3.53, and 4.49 cps for the 82.5° wing and at frequencies of 0.54, 0.96, 1.97, 3.865, and 4.49 cps for the 75° delta wing. Corresponding values of the reduced frequency parameter $\omega b/2V$ for the 82.5° wing are 0.018, 0.034, 0.047, 0.066, and 0.084 and are 0.018, 0.032, 0.066, 0.131, and 0.152 for the 75° wing. Also, at a reduced frequency of about 0.066, oscillation tests of both wings were made for additional amplitudes of 2°, 4°, 8°, and 10° throughout the angle-of-attack range.

For each amplitude, frequency, and angle-of-attack condition, the effects of inertia of the model were eliminated from the data by subtracting wind-off from wind-on results.

The reduced frequency of approximately 0.066 was chosen to correspond closely to one of the frequencies (0.065) of reference 3 for comparison of the 82.5° and 75° wings of the present investigation with the 60° wing discussed in reference 3.

RESULTS AND DISCUSSION

Presentation of Results

The lift, drag, and pitching-moment data for the six delta wings are shown in figure 6 as functions of angle of attack. The static lateral stability derivatives for these wings are plotted against angle of attack and are shown in figure 7, and plots of C_Y, C_l, and C_n against β at several high angles of attack are shown in figures 8, 9, and 10 for the 86.5°, 82.5°, and 75° delta wings. The oscillatory derivatives for the 82.5° and 75° wings are shown in figures 11 to 34, and comparisons of the data obtained for the 82.5° and 75° wings with that obtained for the 60° wing (ref. 3) are shown in figure 35.

Static Characteristics

The lift, drag, and pitching-moment data for all the wings presented in figure 6 show no unusual or unexpected characteristics. The static lateral stability derivatives presented in figure 7 were obtained from the values of the coefficients at $\beta = \pm5°$ for comparison purposes and

do not necessarily represent the slopes through $\beta = 0$, especially, at the high angles of attack where nonlinearities occur in the data. The static-lateral-stability data shown in figure 7 are as might be expected (refs. 5 and 6) with the static stability derivatives for the 86.5° and 82.5° wings showing the large and erratic changes that occur for low-aspect-ratio lifting surfaces at medium and high angles of attack. These large and erratic changes in static lateral stability derivatives at medium and large angles of attack indicate that nonlinearities may exist when the lateral and directional coefficients are plotted against angle of sideslip. These nonlinearities do exist for the 86.5°, 82.5°, and 75° delta wings as is shown in figures 8, 9, and 10, respectively. As can be seen from the figures, the variation of C_Y, C_n, and C_l with β is extremely nonlinear for both the 86.5° and the 82.5° delta wings. In order to see how these nonlinearities affect the oscillatory characteristics of the wings, the 82.5° and 75° wings were oscillated in yaw and the results are discussed in the following sections.

Oscillatory Characteristics

Effective dihedral.- The variation of the effective dihedral parameter $C_{l_{\beta,\omega}} + k^2 C_{l_{\dot{r},\omega}}$ with angle of attack for the 82.5° and 75° delta wings is given in figures 11 and 12 for the different frequencies of oscillation and an amplitude of ±6°. For both wings, the parameter is zero or nearly zero at zero angle of attack and becomes more negative as the angle of attack is increased. The values of $C_{l_{\beta,\omega}} + k^2 C_{l_{\dot{r},\omega}}$ for the 82.5° wing at angles near 30° are appreciably more negative than those obtained for the 75° wing. Also shown in figures 11 and 12 are the static values of C_{l_β} (per radian) for comparison with the oscillatory values of $C_{l_{\beta,\omega}} + k^2 C_{l_{\dot{r},\omega}}$. The comparison shows that the static C_{l_β} values for both wings exhibit the same trend with angle of attack as is shown by the oscillatory derivatives. A comparison of the variation of $C_{l_{\beta,\omega}} + k^2 C_{l_{\dot{r},\omega}}$ with angle of attack for the 82.5°, 75°, and 60° wings is given in figure 35(a) for a reduced frequency $\frac{\omega b}{2V}$ of about 0.066 and an amplitude ψ_o of ±6°. The figure shows that while at low angles of attack the values of the parameter are nearly the same for all the wings; above an angle of attack of about 10° the curves diverge and the value of the parameter at 30° is close to zero for the 60° wing, about -0.4 for the 75° wing, and about -0.7 for the 82.5° wing.

In order to show the effect of frequency on the parameter $C_{l_{\beta,\omega}} + k^2 C_{l_{\dot{r},\omega}}$, cross plots of figures 11 and 12 were made for a number

of angles of attack and are presented in figures 13 and 14. Generally for the low angles of attack presented there is only a small effect of frequency on $Cl_{\beta,\omega} + k^2 Cl_{\dot{r},\omega}$ for both the 82.5° and 75° wings. At the higher angles of attack, there appears to be no consistent effect of frequency, although for the 75° wing the values of $Cl_{\beta,\omega} + k^2 Cl_{\dot{r},\omega}$ become more negative with an increase in frequency.

Large variations of $Cl_{\beta,\omega} + k^2 Cl_{\dot{r},\omega}$ with amplitude were obtained at the high angles for both wings (figs. 15 and 16), and the changes were usually greater for the 82.5° wing.

Directional stability.- The variation of the directional stability parameter $Cn_{\beta,\omega} + k^2 Cn_{\dot{r},\omega}$ with angle of attack for the 82.5° and 75° wings is given in figures 17 and 18 for different values of the reduced frequency parameter $\frac{\omega b}{2V}$ and for an amplitude ψ_o of ±6°. Figure 17 shows that for all frequencies the parameter is small and negative at zero angle of attack for the 82.5° wing, becomes more negative with angle of attack up to about 20°, after 20° becomes less negative, and at angles of attack above 40° the values of the parameter become positive. The value of the parameter at 0° angle of attack for the 75° wing is zero or a small negative value, depending on the frequency. (See fig. 18.) At some small positive angle the parameter assumes a small positive value which is more or less constant up to about 30° angle of attack; above 30° angle of attack, however, the values of $Cn_{\beta,\omega} + k^2 Cn_{\dot{r},\omega}$ become negative. Also shown in figures 17 and 18 are the static values of Cn_β (per radian) which can be compared with the oscillatory values of $Cn_{\beta,\omega} + k^2 Cn_{\dot{r},\omega}$. The comparison shows, as was noted for Cl_β, that the static values of Cn_β for both wings exhibit the same trend with angle of attack as is shown by the oscillatory derivatives. A comparison of the variation of $Cn_{\beta,\omega} + k^2 Cn_{\dot{r},\omega}$ with angle of attack for the 60°, 75°, and 82.5° wings for a reduced frequency of about 0.066 and an amplitude ψ_o of ±6° is shown in figure 35(a).

Both the 60° and 75° wings have small positive values of the derivative at small angles of attack up to about 10°, whereas the 82.5° wing has relatively large negative values indicating directional instability. At an angle of attack of about 22°, the 75° wing still has a small positive value, and the 60° wing has a positive value about $1\frac{1}{2}$ times that of the 75° wing while the 82.5° wing has a large negative value which is about 5 times that of the 60° wing.

The variation of $C_{n_{\beta,\omega}} + k^2 C_{n_{\dot{r},\omega}}$ with reduced frequency $\frac{\omega b}{2V}$ for the 82.5° wing is irregular even at 0° angle of attack while the variation of the parameter with frequency is generally very small for the 75° wing except for 40° and 50° angles of attack. (See figs. 19 and 20.)

Extremely large values and large variations of $C_{n_{\beta,\omega}} + k^2 C_{n_{\dot{r},\omega}}$ with amplitude were obtained for the 82.5° wing especially at the higher angles of attack, as is shown on figure 21, for a reduced frequency $\frac{\omega b}{2V}$ of 0.066. For example, at an angle of attack of 50° the values varied from about -0.32 at 2° amplitude to about 0.64 at 6° amplitude. The values of the parameter for the 75° wing were considerably smaller in magnitude (fig. 22), and the variation with amplitude was generally very small; however, a large change in the parameter occurred between 2° and 4° amplitude for 40° and 50° angles of attack where the values of the parameter changed from a positive to a negative value.

Rolling moment due to yawing.- The variation with angle of attack of the rolling moment due to yawing $C_{l_{r,\omega}} - C_{l_{\dot{\beta},\omega}}$ for the 82.5° and 75° wings is given in figures 23 and 24.

For the 82.5° wing, the variation with angle of attack is nonlinear, the values being positive in the low-angle-of-attack range and becoming large negative values above about 22° and becoming positive or tending to become positive at angles of attack above 30°. For the low frequencies, the values of $C_{l_{r,\omega}} - C_{l_{\dot{\beta},\omega}}$ for the 75° wing are negative in the low-angle-of-attack range while at the higher frequencies the values are small and positive. At angles of attack above about 30°, the variation becomes extremely nonlinear for the three lower frequencies and the values of the parameter are positive in the range around 40° angle of attack.

Figure 35(b) shows a comparison of the values of $C_{l_{r,\omega}} - C_{l_{\dot{\beta},\omega}}$ for the 82.5°, 75°, and 60° delta wings for a reduced frequency $\frac{\omega b}{2V}$ of 0.066 and ±6° amplitude. The figure shows that, even though there is only a small difference in the values of $C_{l_{r,\omega}} - C_{l_{\dot{\beta},\omega}}$ for the three wings at low angles of attack, there is a large difference in the angle-of-attack range above 24° and at an angle of attack of 30° increasing the sweep of the leading edge from 60° to 82.5° changes the value of the parameter from 2.8 to -2.6.

The effects of frequency on the parameter $C_{l_{r,\omega}} - C_{l_{\dot{\beta},\omega}}$ are shown in figures 25 and 26 which are cross plots of figures 23 and 24, respectively. The 82.5° wing shows less variation of the parameter with

frequency in the low-angle-of-attack range than does the 75° wing. At the high angles of attack the effects of frequency or the value of $C_{l_{r,\omega}} - C_{l_{\dot{\beta},\omega}}$ for both wings are considerably greater than at the the lower angles of attack.

The variation of $C_{l_{r,\omega}} - C_{l_{\dot{\beta},\omega}}$ with amplitude for both wings is shown in figures 27 and 28. The figures show that amplitude has a large effect on the magnitude of the parameter for the 82.5° wing at all angles of attack shown except 0° angle of attack. For the 75° wing, a much smaller effect of amplitude can be noted in figure 28.

Damping in yaw.- The variation with angle of attack of the damping-in-yaw parameter $C_{n_{r,\omega}} - C_{n_{\dot{\beta},\omega}}$ for the 82.5° and 75° wings is given in figures 29 and 30. The damping in yaw for the 82.5° wing is zero or slightly negative up to about 10° angle of attack and becomes more negative up to about 20°, but after 20° the variation with angle of attack is irregular and depends on frequency. For the 75° wing (fig. 30), the value of the parameter is zero or nearly zero to about 20°; after 20° the values become large and negative up to about 40° and then tend to become less negative. Figure 35(b) shows a comparison of the variation of $C_{n_{r,\omega}} - C_{n_{\dot{\beta},\omega}}$ for the 60°, 75°, and 82.5° wings. For all three wings, $C_{n_{r,\omega}} - C_{n_{\dot{\beta},\omega}}$ is nearly zero in the low-angle-of-attack range, as was expected, and the values become more negative at higher angles of attack. In the range around 20° angle of attack, the 82.5° wing has the greatest negative values.

Figures 31 and 32 show the variation with frequency of $C_{n_{r,\omega}} - C_{n_{\dot{\beta},\omega}}$ for the 82.5° and 75° wings for several angles of attack and an amplitude of ±6°. For both wings at low angles of attack, the effects of frequency are small. The effect of frequency is extremely large and erratic for the 82.5° wing at 30° and 40° but for the 75° wing the variation is extremely large only for an angle of attack of 40°. Similarly, the effect of amplitude is large only at the higher angles of attack presented and generally the largest changes in the parameter occur in the range from between 2° and 4° in amplitude for both the 82.5° and 75° wings. (See figs. 33 and 34.)

CONCLUSIONS

The static lateral stability of six delta wings was determined at subsonic speeds and, in addition, two of the wings with 82.5° and 75° sweep of the leading edge were oscillated in yaw about the 50-percent point of the root chord in order to determine the effects of frequency

and amplitude on the combination lateral stability derivatives resulting from this motion. The results of this investigation indicate the following conclusions:

1. The results of the oscillation tests showed that large changes in the derivatives occurred with changes of frequency and amplitude at the high angles of attack for the 82.5° and 75° delta wings. For the reduced frequency parameter $\frac{\omega b}{2V} = 0.066$ the largest changes in the derivatives with amplitude generally occurred at low values of amplitude.

2. Comparison of the variation with angle of attack of the oscillatory derivatives obtained with the 82.5° and 75° wing with those of a 60° wing of another investigation showed that large differences in the oscillatory derivatives are generally obtained at the higher angles of attack and that the values of the combination oscillatory derivatives $C_{n_{\beta,\omega}} + k^2 C_{n_{\dot{r},\omega}}$ and $C_{l_{r,\omega}} - C_{l_{\dot{\beta},\omega}}$ for the 82.5° wing are very large and of opposite sign to those of the other wings. This comparison was made for one frequency and amplitude of oscillation.

3. The results of the static tests showed that the static lateral stability derivatives followed trends which were similar to those of other investigations.

Langley Aeronautical Laboratory,
National Advisory Committee for Aeronautics,
Langley Field, Va., January 7, 1957.

REFERENCES

1. Campbell, John P., and Woodling, Carroll H.: Calculated Effects of the Lateral Acceleration Derivatives on the Dynamic Lateral Stability of a Delta-Wing Airplane. NACA RM L54K26, 1955.

2. Campbell, John P., Johnson, Joseph L., Jr., and Hewes, Donald E.: Low-Speed Study of the Effect of Frequency on the Stability Derivatives of Wings Oscillating in Yaw With Particular Reference to High Angle-of-Attack Conditions. NACA RM L55H05, 1955.

3. Fisher, Lewis R.: Experimental Determination of the Effects of Frequency and Amplitude on the Lateral Stability Derivatives for a Delta, a Swept, and an Unswept Wing Oscillating in Yaw. NACA RM L56A19, 1956.

4. Queijo, M. J., Fletcher, Herman S., Marple, C. G., and Hughes, F. M.: Preliminary Measurements of the Aerodynamic Yawing Derivatives of a Triangular, a Swept, and an Unswept Wing Performing Pure Yawing Oscillations, With a Description of the Instrumentation Employed. NACA RM L55L14, 1956.

5. Tosti, Louis P.: Low-Speed Static Stability and Damping-in-Roll Characteristics of Some Swept and Unswept Low-Aspect-Ratio Wings. NACA TN 1468, 1947.

6. McKinney, Marion O., Jr., and Drake, Hubert M.: Flight Characteristics at Low Speed of Delta-Wing Models. NACA RM L7K07, 1948.

TABLE I

GEOMETRIC CHARACTERISTICS OF SIX DELTA WINGS

	Wing					
	1	2	3	4	5	6
Aspect ratio.	0.25	0.53	1.07	2.31	4.0	6.93
Leading-edge sweep angle, deg . .	86.5	82.5	75	60	45	30
Dihedral angle, deg	0	0	0	0	0	0
Twist, deg	0	0	0	0	0	0
Airfoil section	Flat plate	Flat plate	Flat plate	Flat plate	Flat plate	Flat plate
Area, sq in.	144	207.4	335.8	561.2	703.2	405.9
Span, in.	6	10.45	18.97	36.00	53.03	53.03
Mean aerodynamic chord, in. . . .	32.00	26.46	23.60	20.79	17.68	10.21

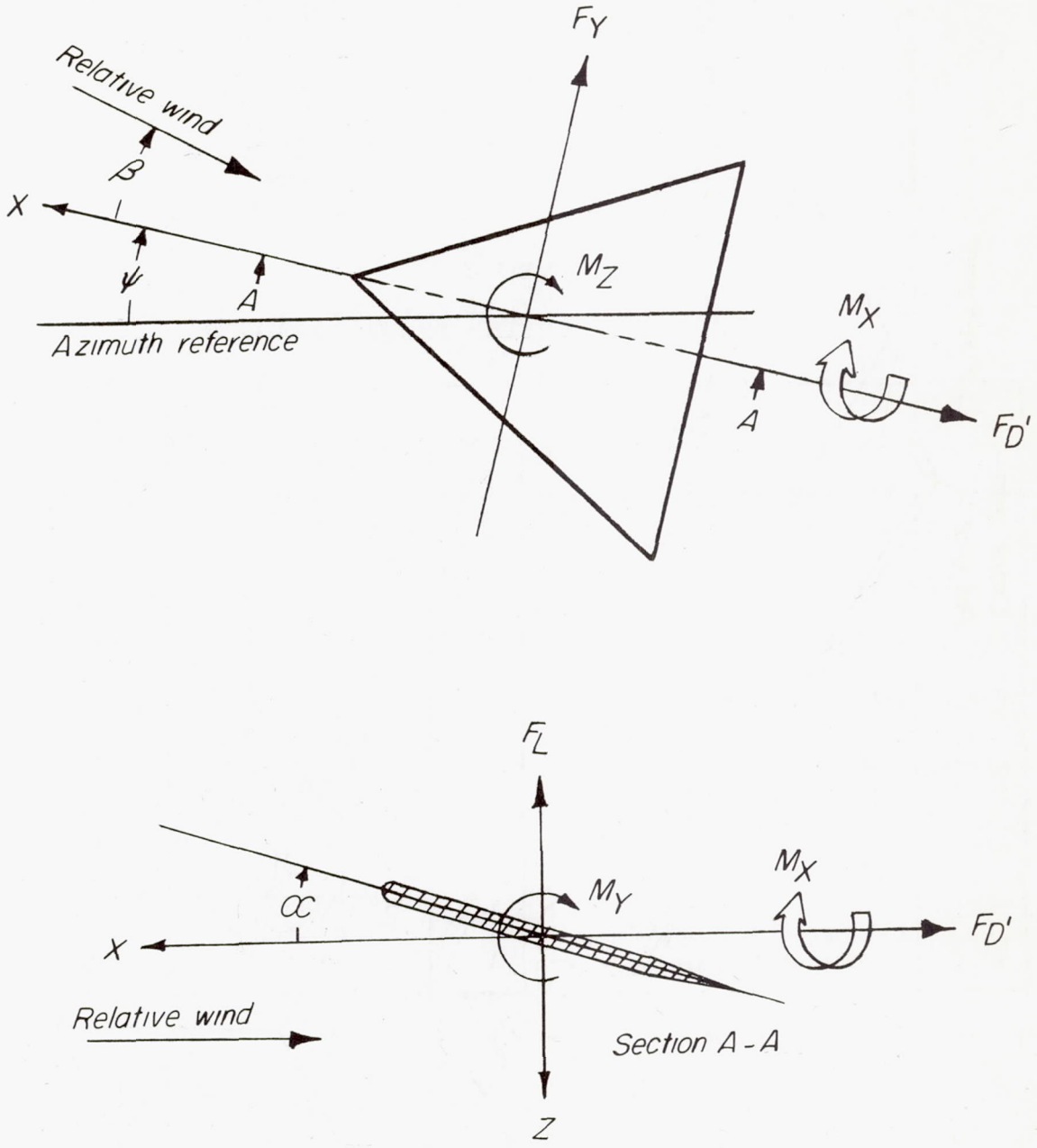

Figure 1.- System of stability axes. Arrows indicate positive forces, moments, and angular displacements.

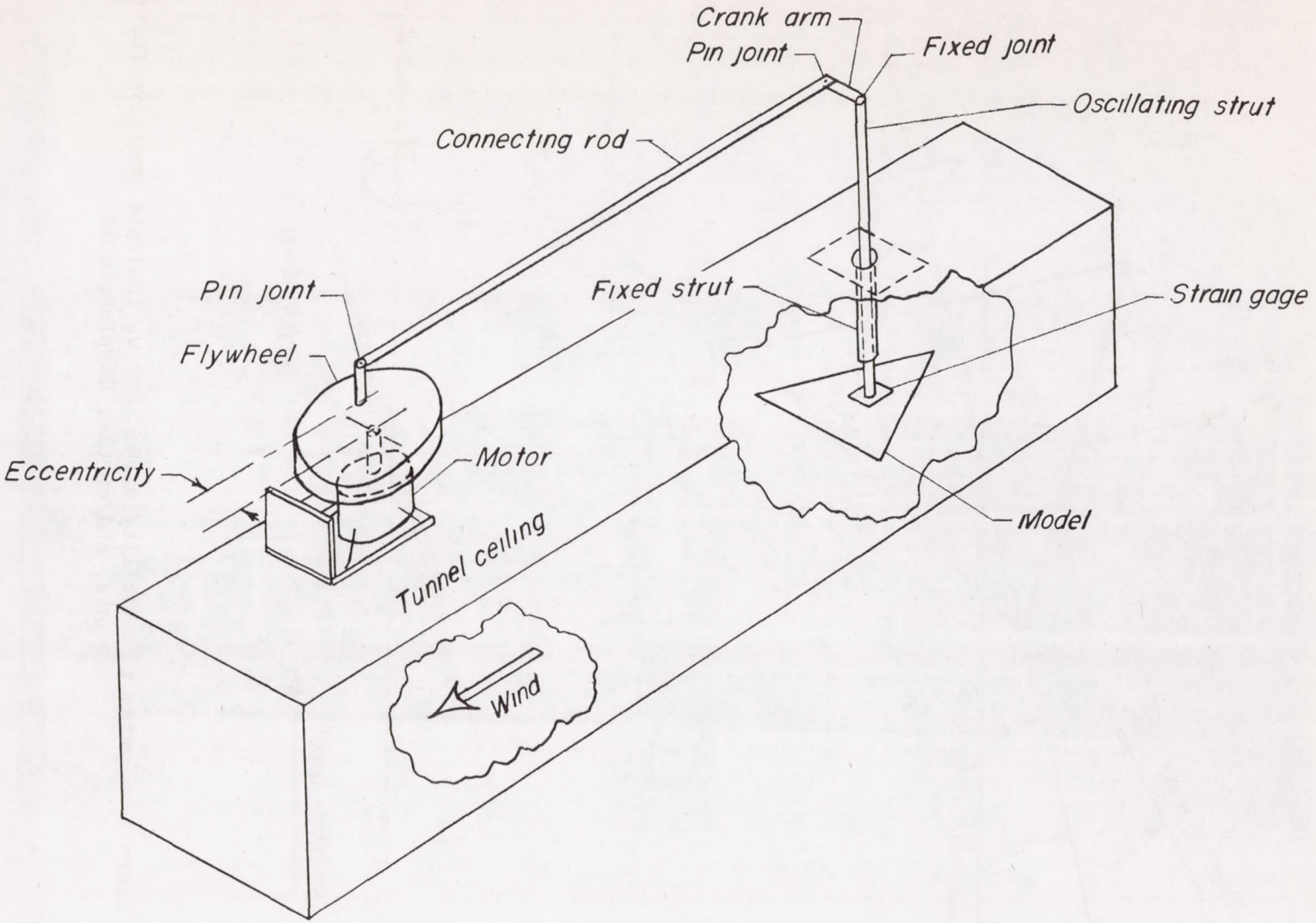

Figure 2.- Sketch of oscillation-in-yaw equipment.

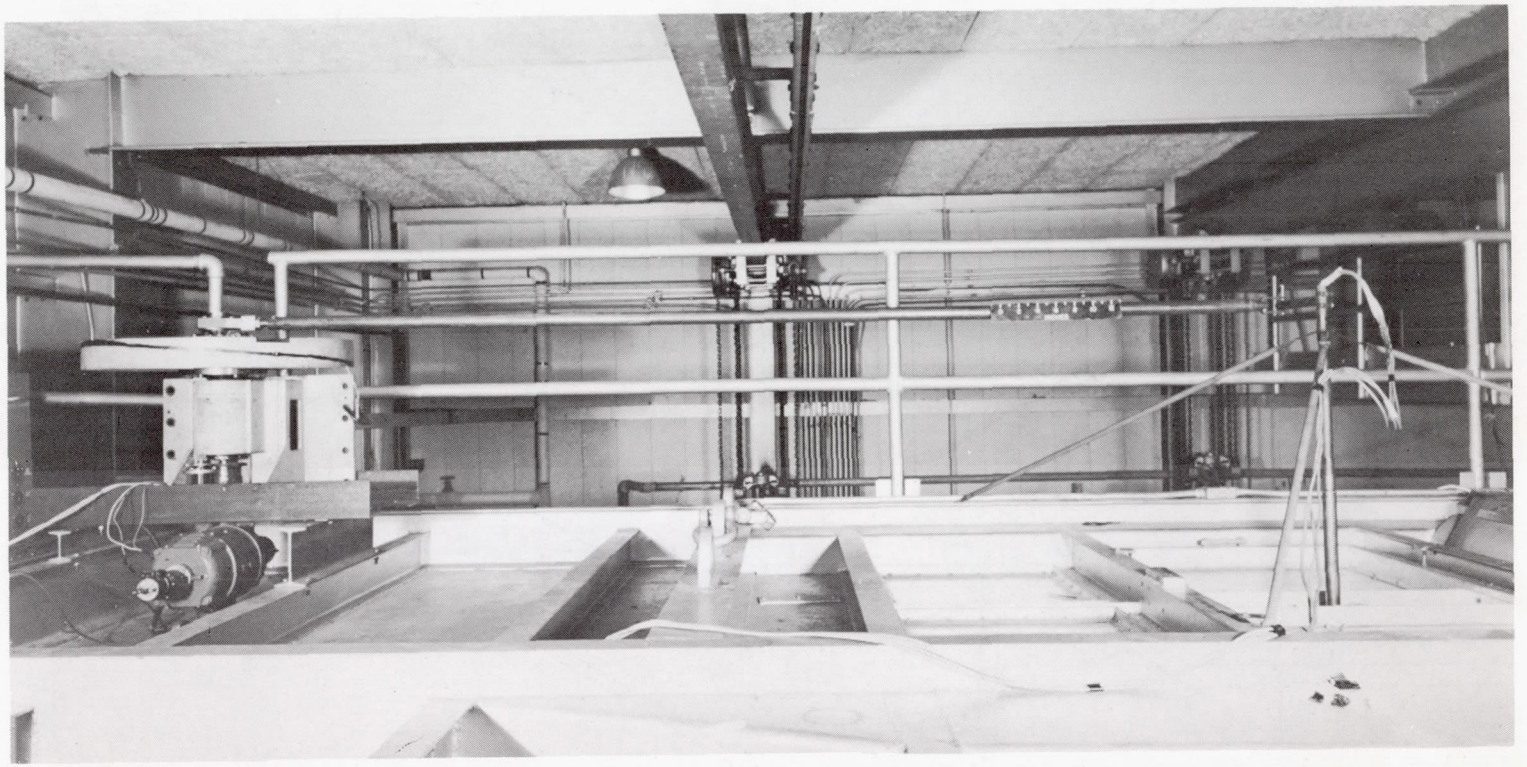

L-90944

Figure 3.- Photograph of oscillation-in-yaw equipment on top of tunnel test section.

(a) 82.5° delta wing. L-91176

Figure 4.- Photographs of models in tunnel.

L-91177

(b) 75° delta wing.

Figure 4.- Concluded.

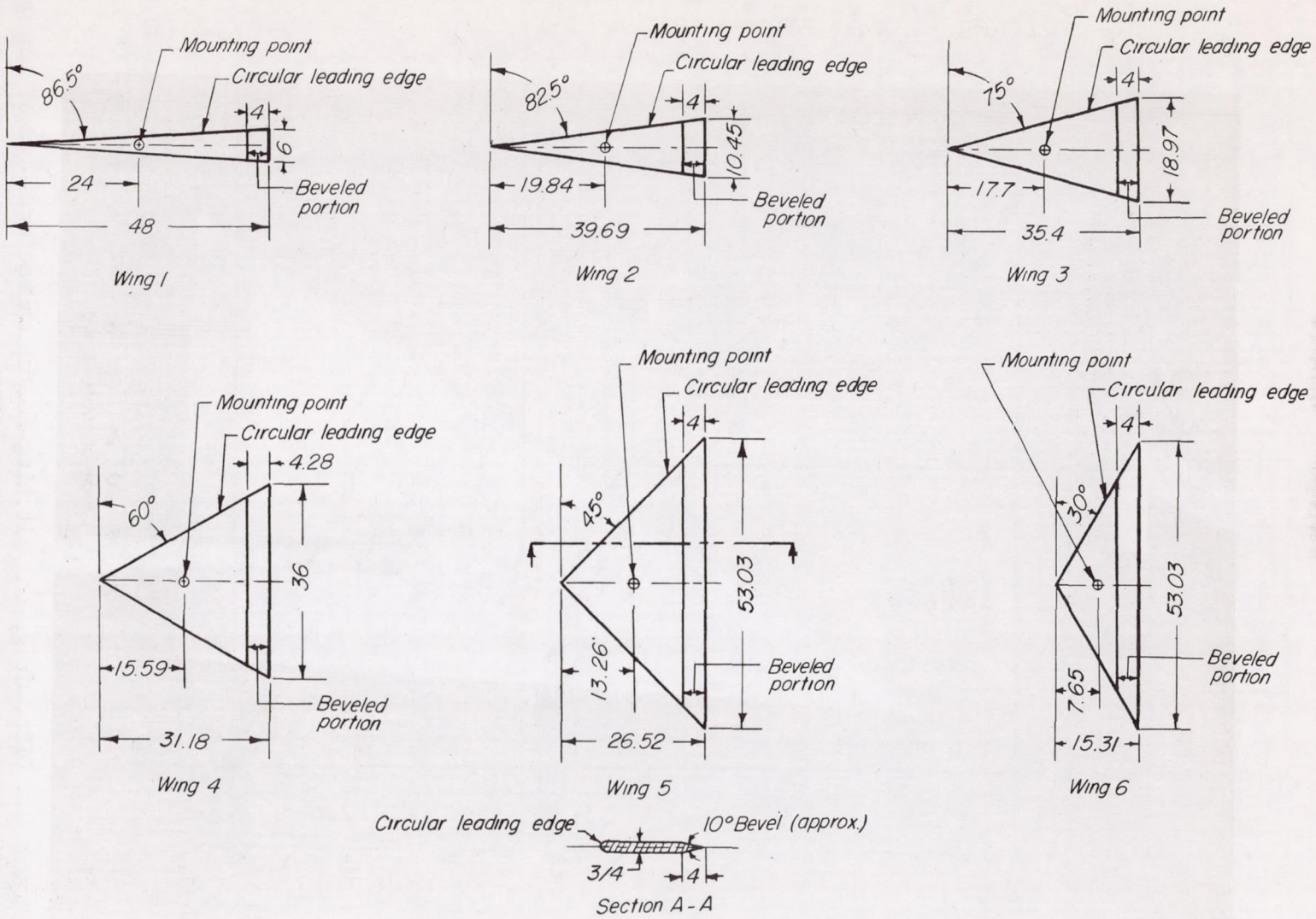

Figure 5.- Sketches of the delta-wing models investigated. All dimensions are in inches.

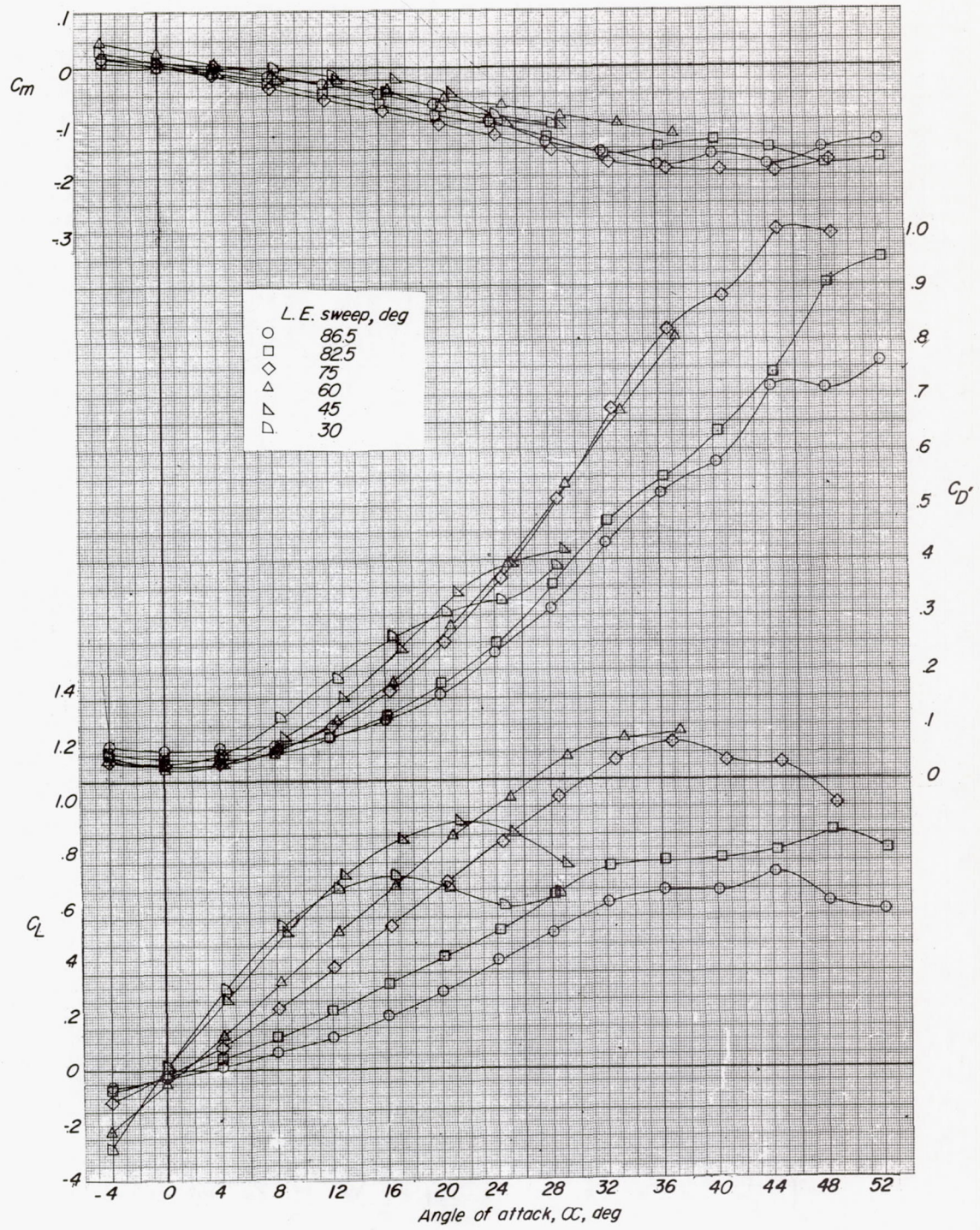

Figure 6.- Lift, drag, and pitching-moment characteristics of the delta wings tested.

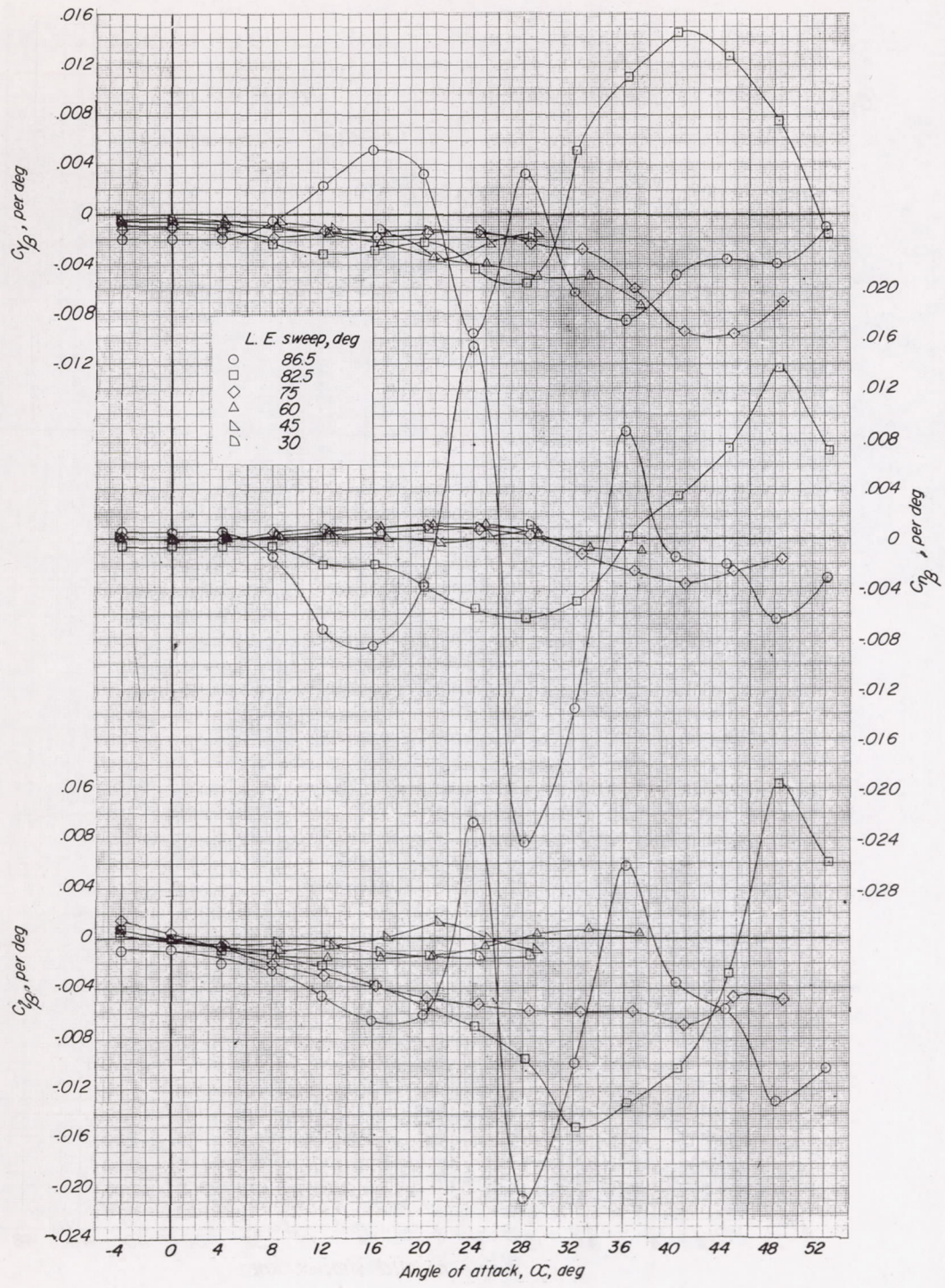

Figure 7.- Static lateral stability derivatives of the delta wings tested.

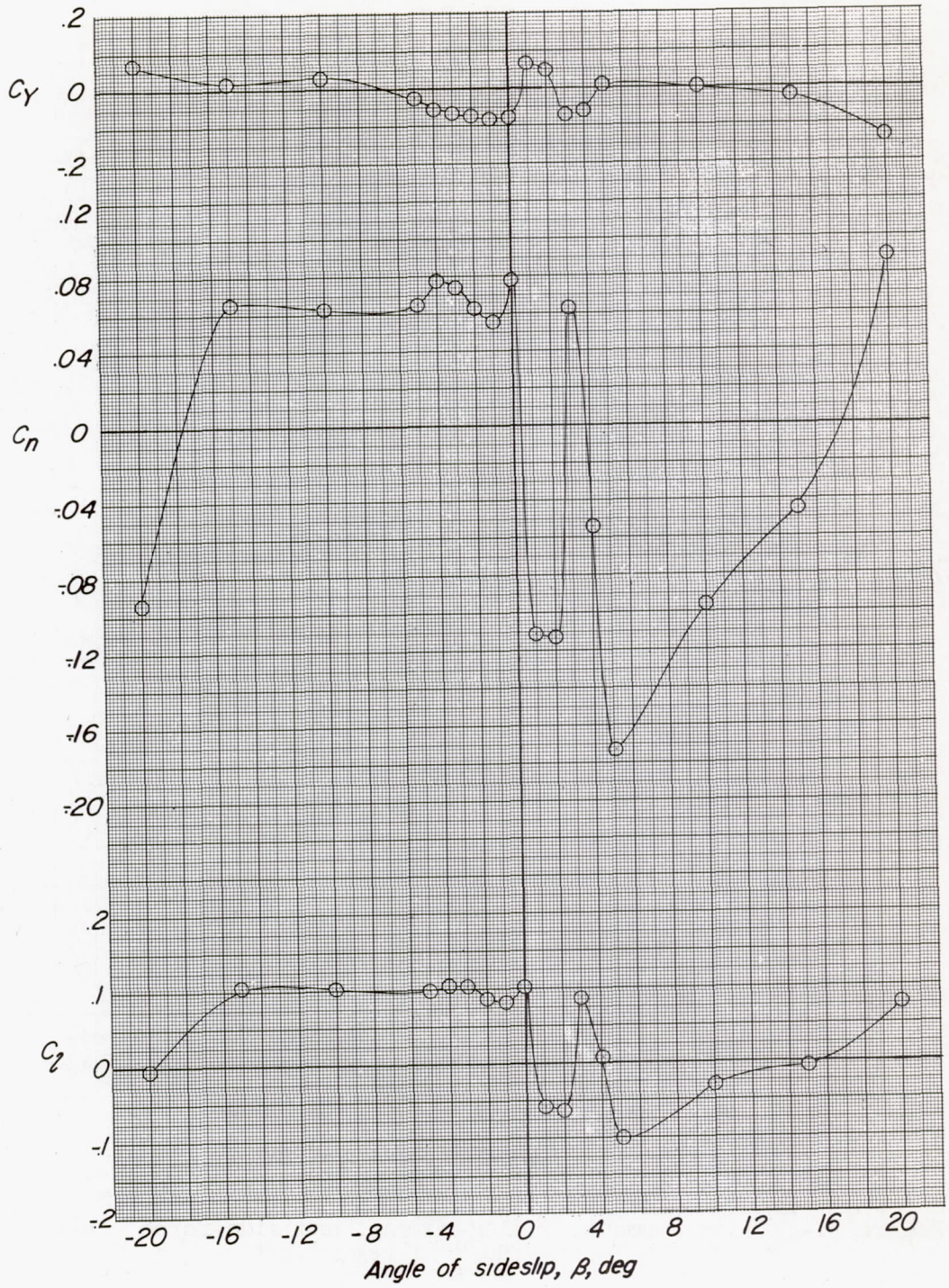

Figure 8.- Rolling-moment, yawing-moment, and side-force characteristics of the 86.5° delta wing at 28° angle of attack.

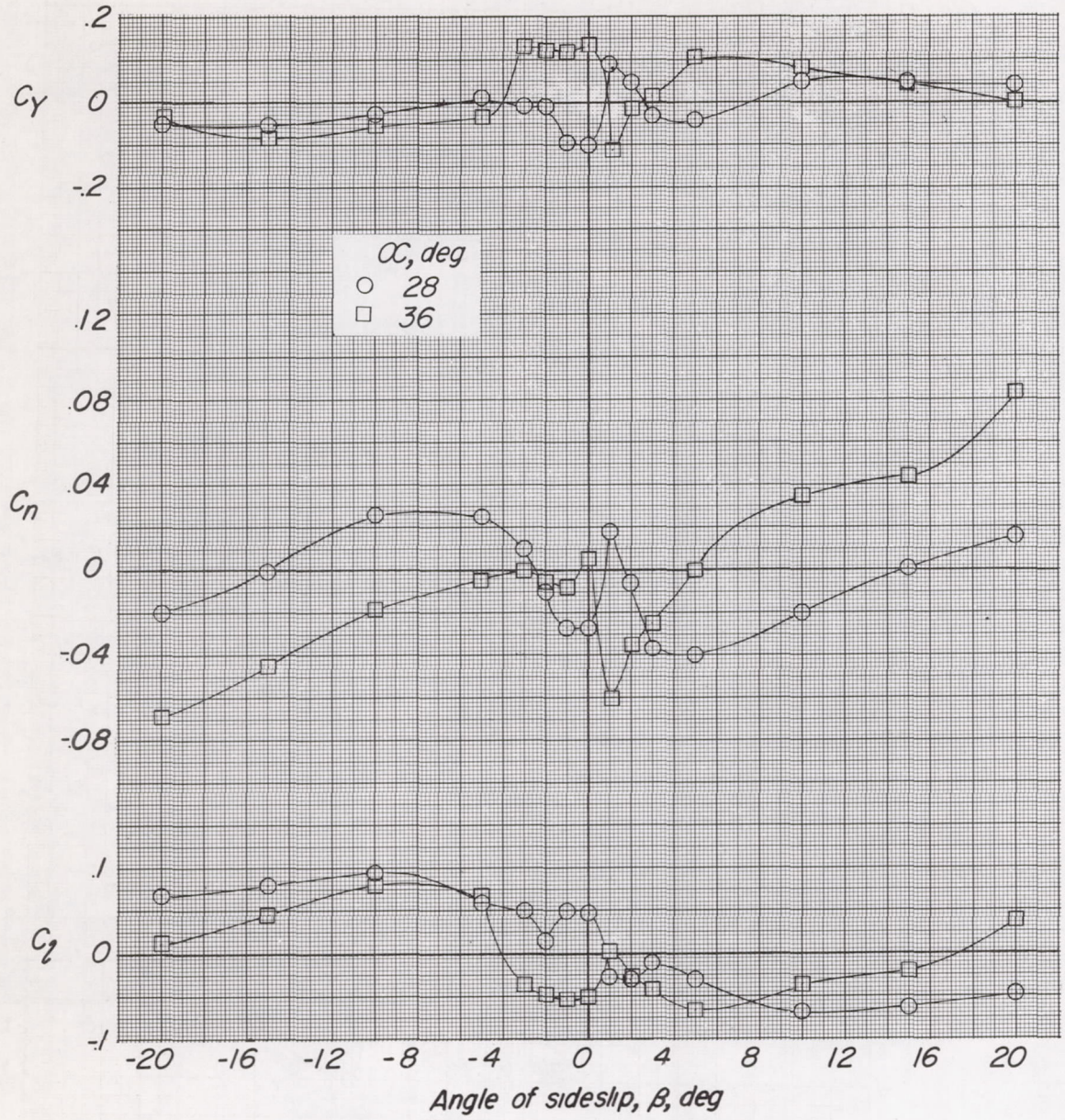

Figure 9.- Rolling-moment, yawing-moment, and side-force characteristics of the 82.5° delta wing.

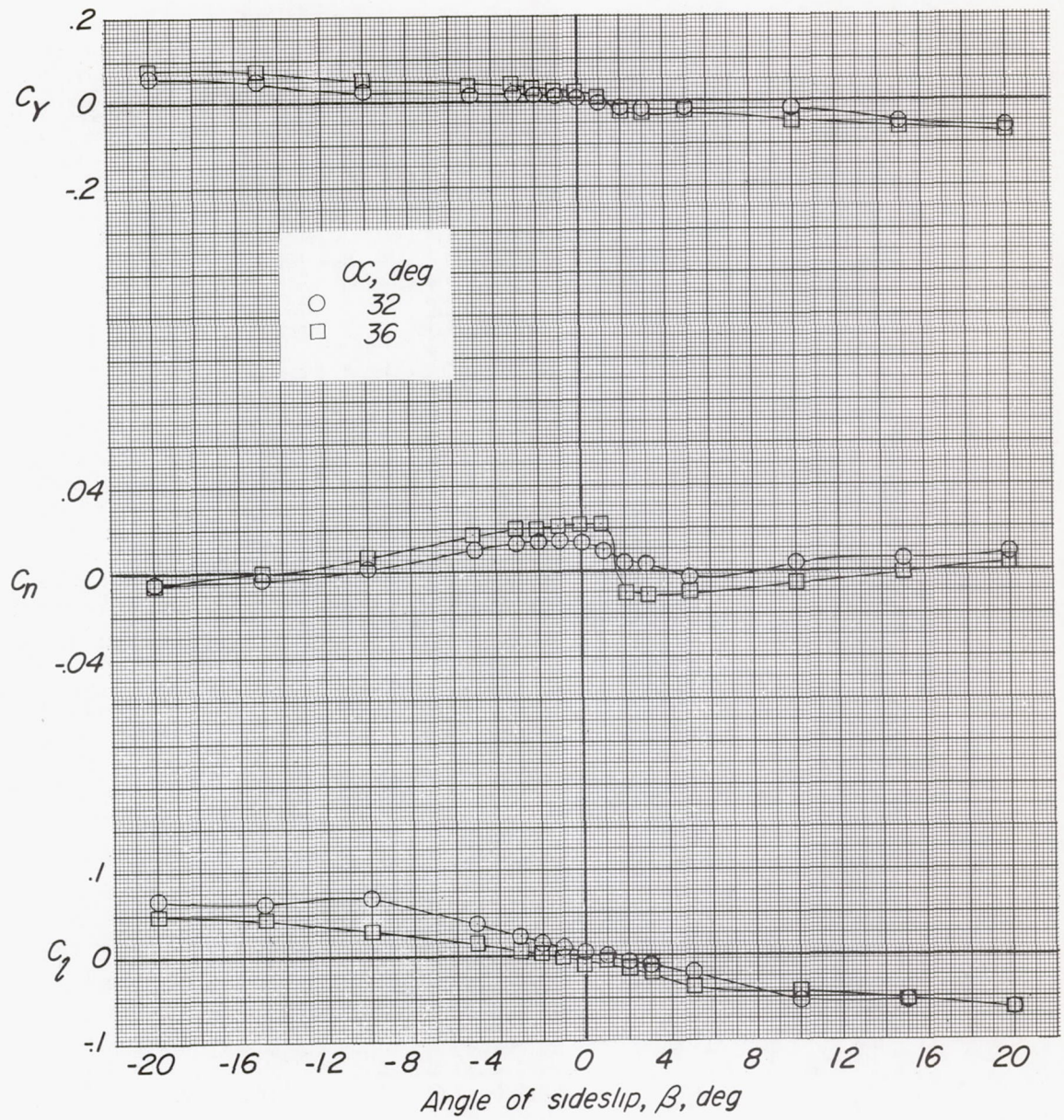

Figure 10.- Rolling-moment, yawing-moment, and side-force characteristics of the 75° delta wing.

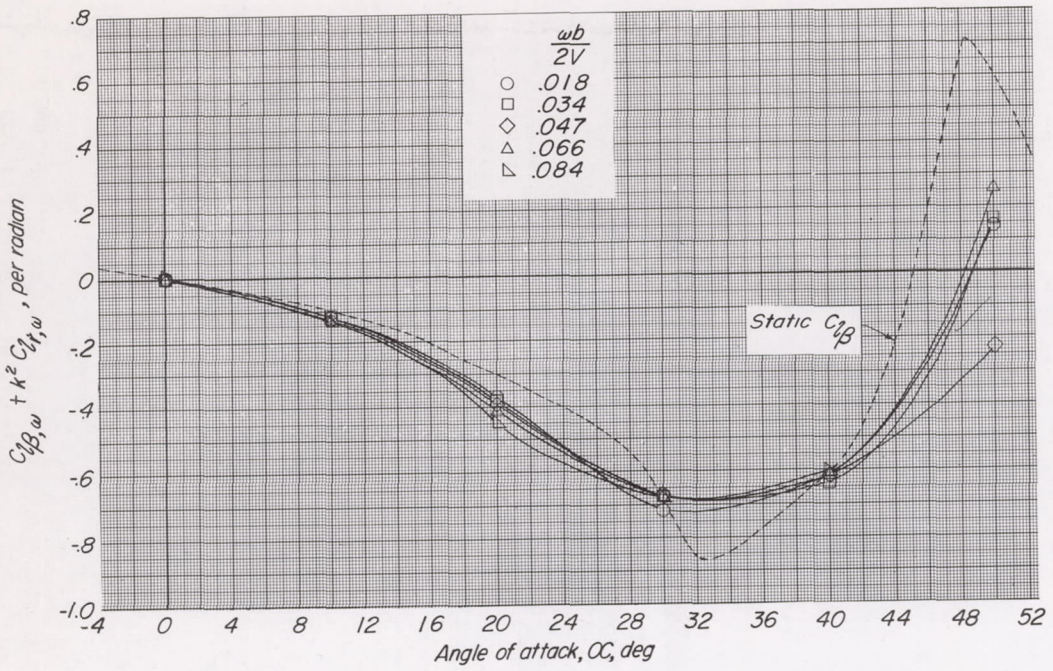

Figure 11.- Variation with angle of attack of the effective dihedral parameter for the 82.5° delta wing measured during oscillation. $\psi_o = \pm 6^\circ$.

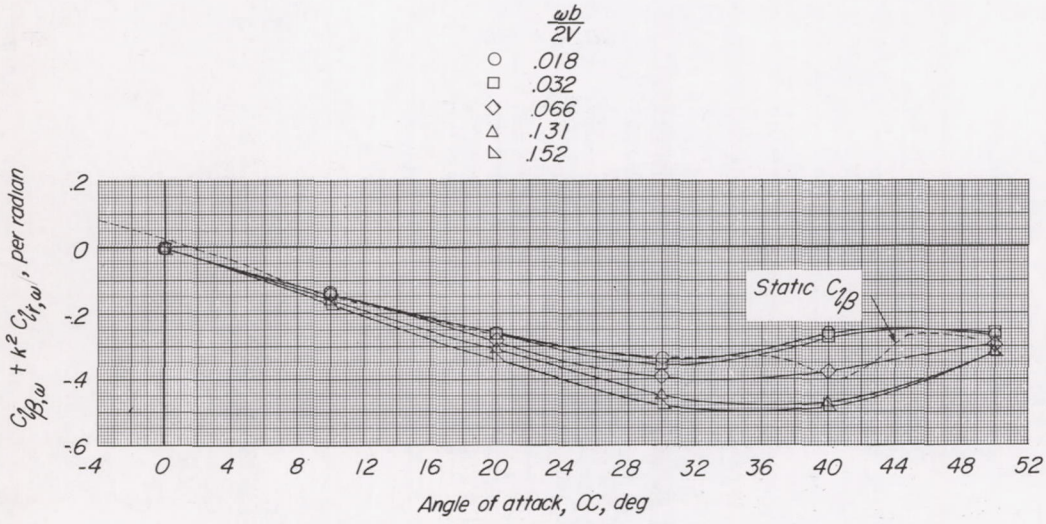

Figure 12.- Variation with angle of attack of the effective dihedral parameter for the 75° delta wing measured during oscillation. $\psi_o = \pm 6^\circ$.

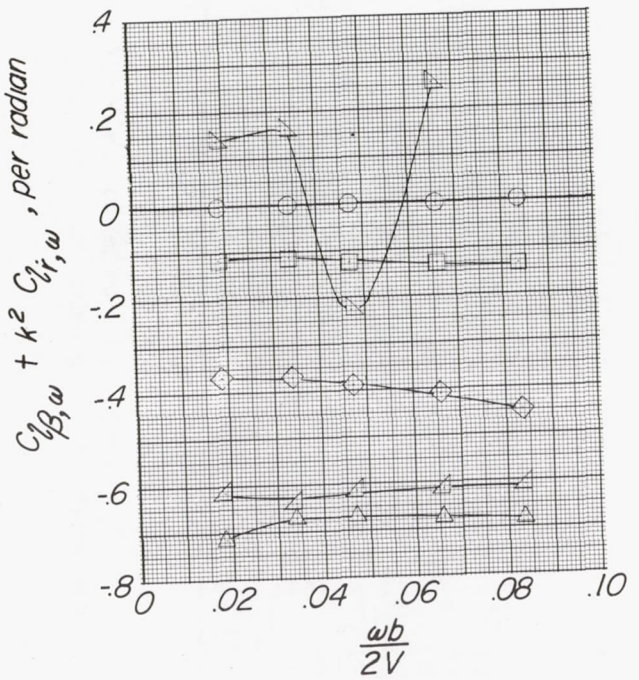

Figure 13.- Variation with frequency parameter of the effective dihedral parameter for the 82.5° delta wing. $\psi_o = \pm 6^o$.

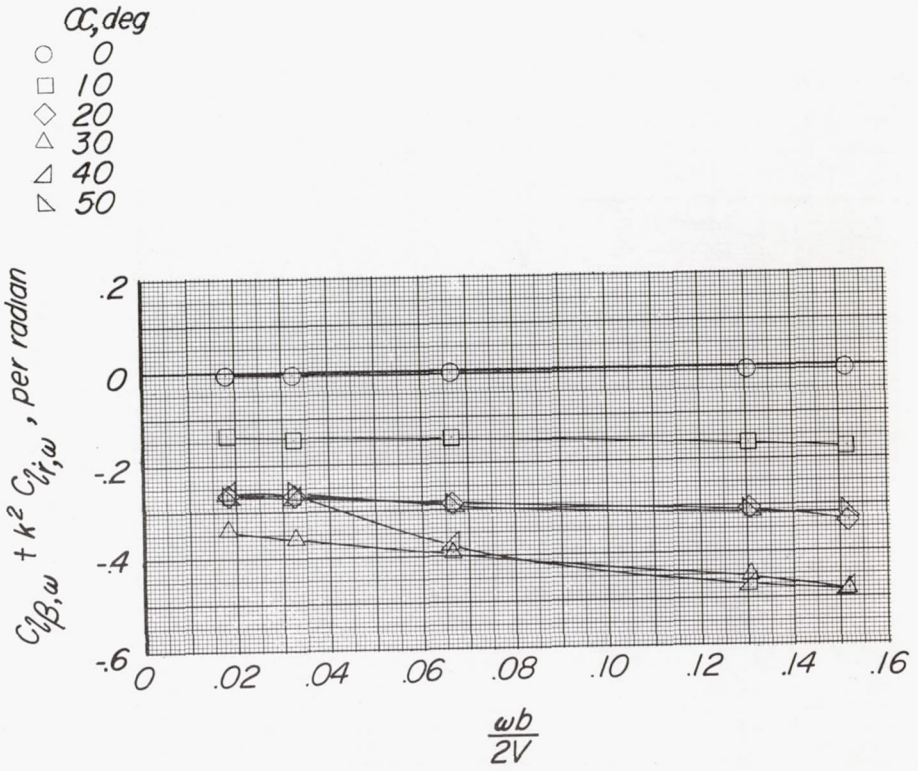

Figure 14.- Variation with frequency parameter of the effective dihedral parameter for the 75° delta wing. $\psi_o = \pm 6^o$.

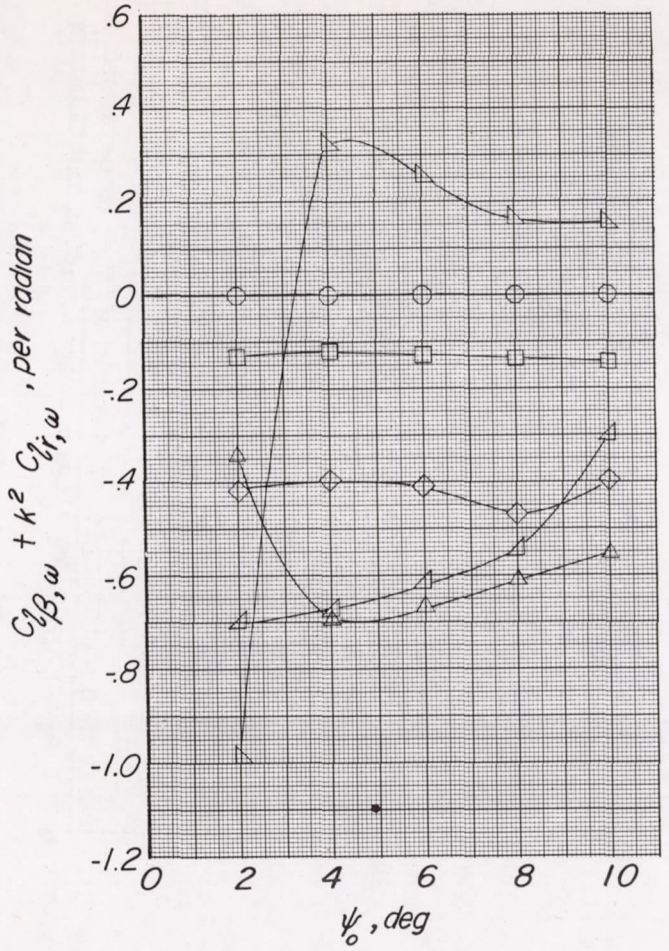

Figure 15.- Variation with amplitude of the effective dihedral parameter for the 82.5° delta wing. $\omega b/2V = 0.066$.

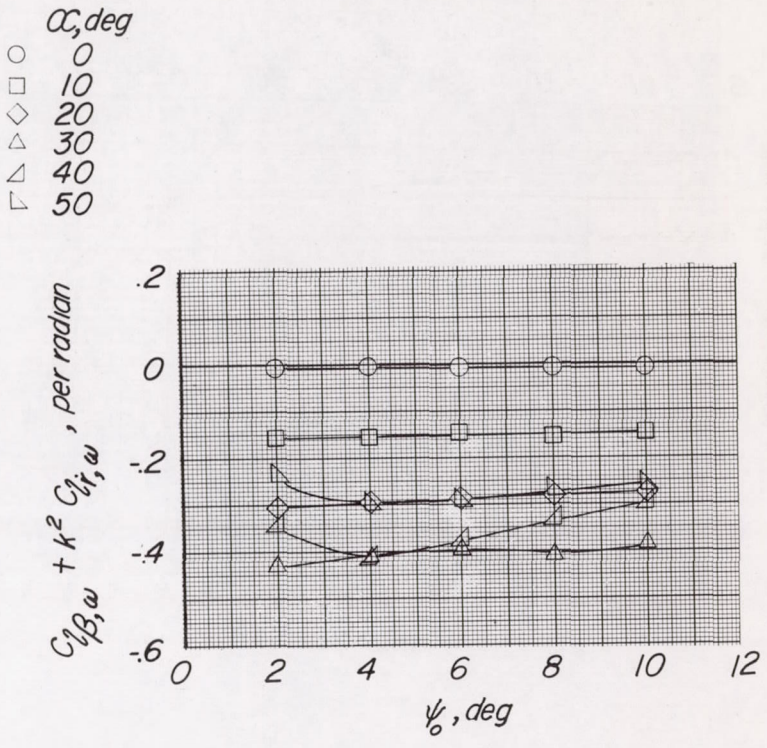

Figure 16.- Variation with amplitude of the effective dihedral parameter for the 75° delta wing. $\omega b/2V = 0.066$.

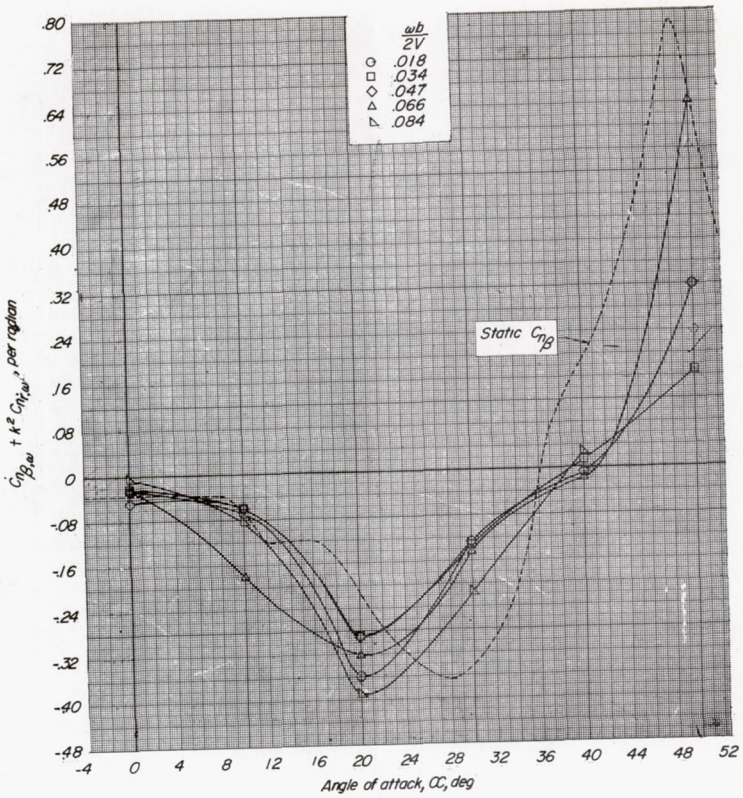

Figure 17.- Variation with angle of attack of the directional stability parameter for the 82.5° delta wing measured during oscillation. $\psi_o = \pm 6^\circ$.

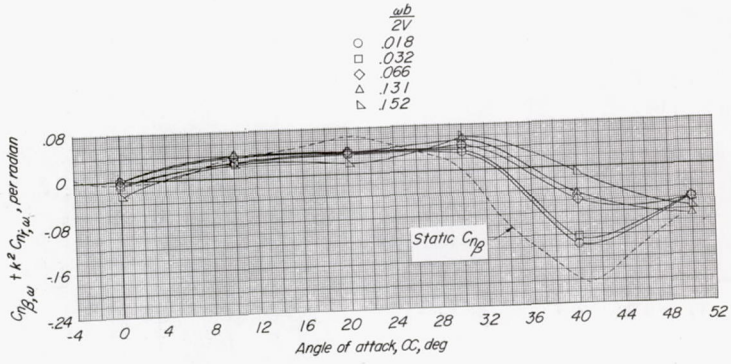

Figure 18.- Variation with angle of attack of the directional stability parameter for the 75° delta wing measured during oscillation. $\psi_o = \pm 6^\circ$.

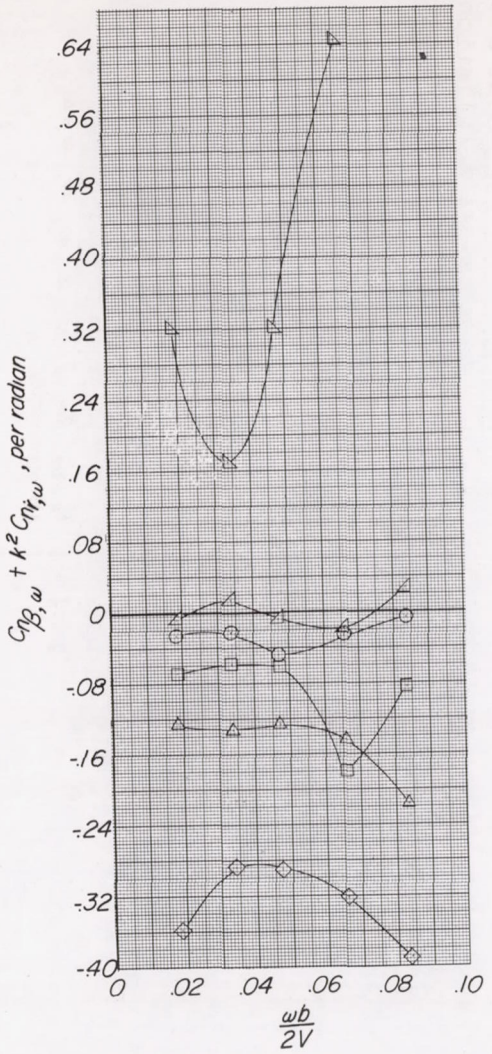

Figure 19.- Variation with frequency parameter of the directional stability parameter for the 82.5° delta wing. $\psi_o = \pm 6^o$.

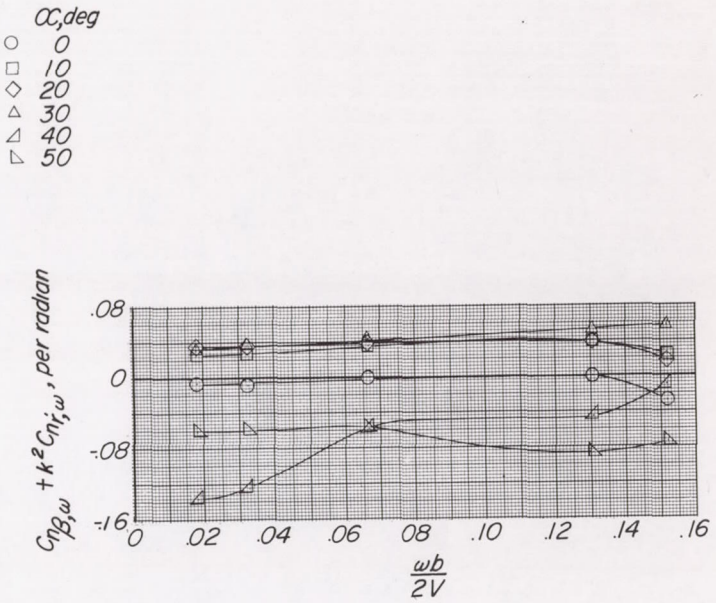

Figure 20.- Variation with frequency parameter of the directional stability parameter for the 75° delta wing. $\psi_o = \pm 6^o$.

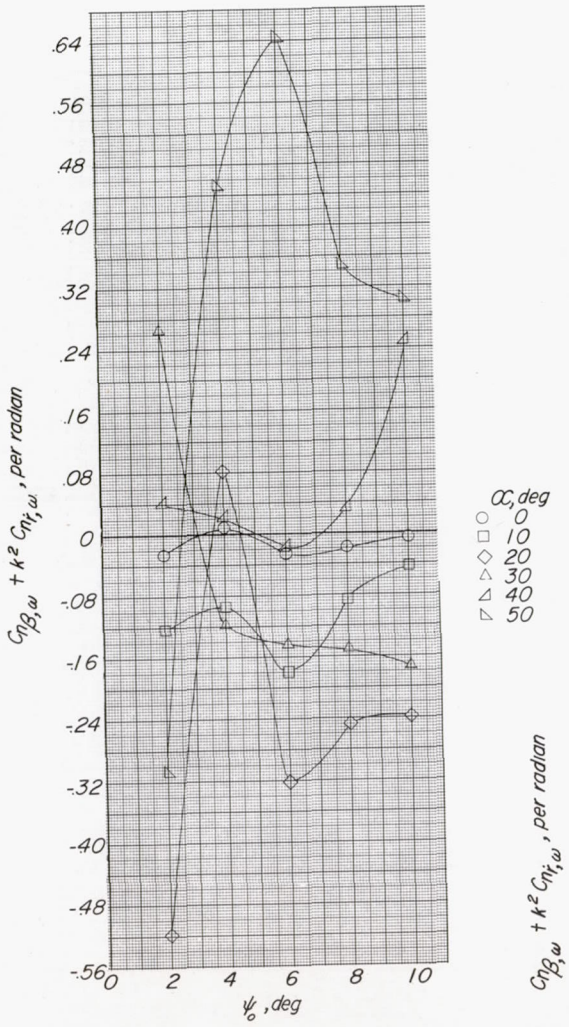

Figure 21.- Variation with amplitude of the directional stability parameter for the 82.5° delta wing. $\omega b/2V = 0.066$.

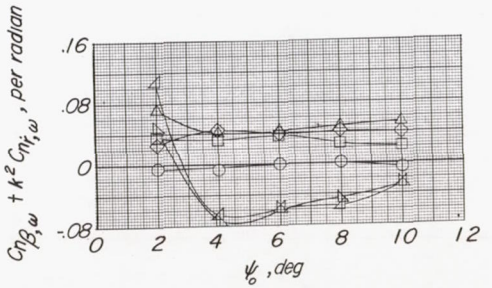

Figure 22.- Variation with amplitude of the directional stability parameter for the 75° delta wing. $\omega b/2V = 0.066$.

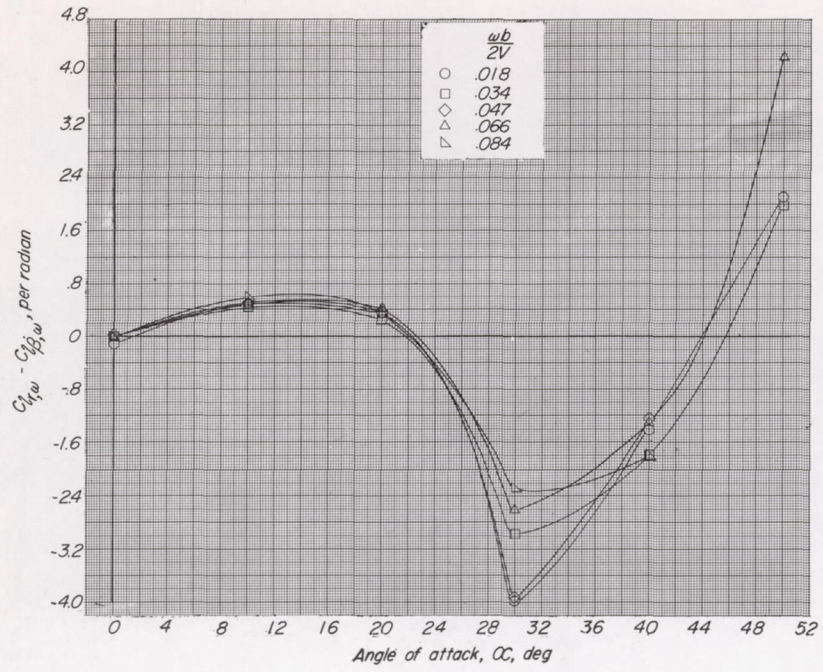

Figure 23.- Variation with angle of attack of the rolling moment due to yawing parameter for the 82.5° delta wing measured during oscillation. $\psi_o = \pm 6^\circ$.

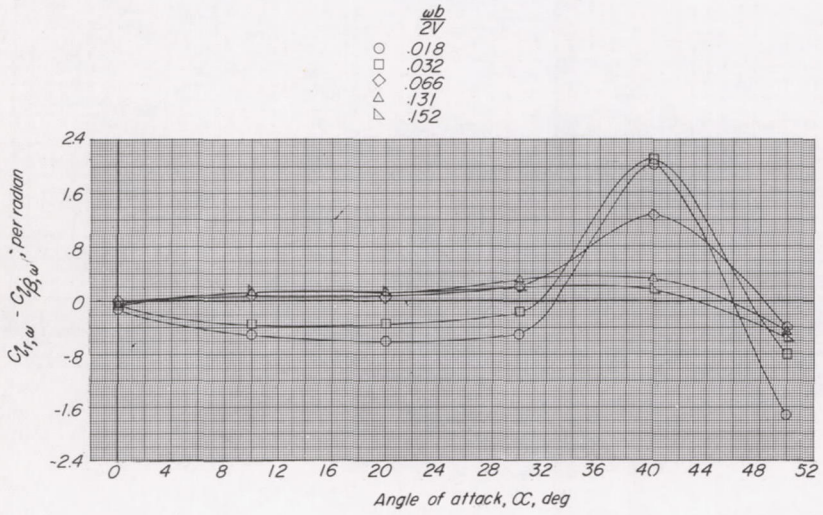

Figure 24.- Variation with angle of attack of the rolling moment due to yawing parameter for the 75° delta wing measured during oscillation. $\psi_o = \pm 6^\circ$.

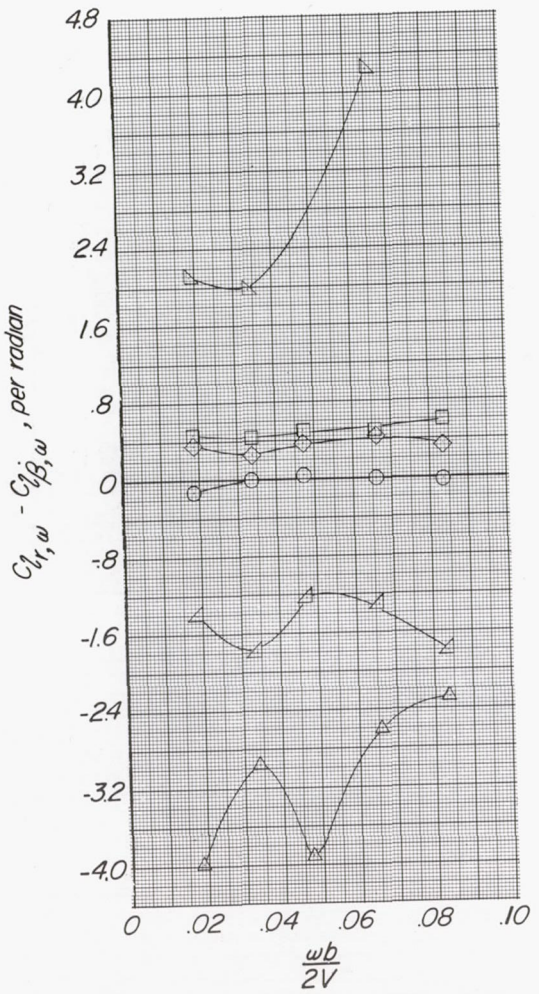

Figure 25.- Variation with frequency parameter of the rolling moment due to yawing parameter for the 82.5° delta wing. $\psi_o = \pm 6^o$.

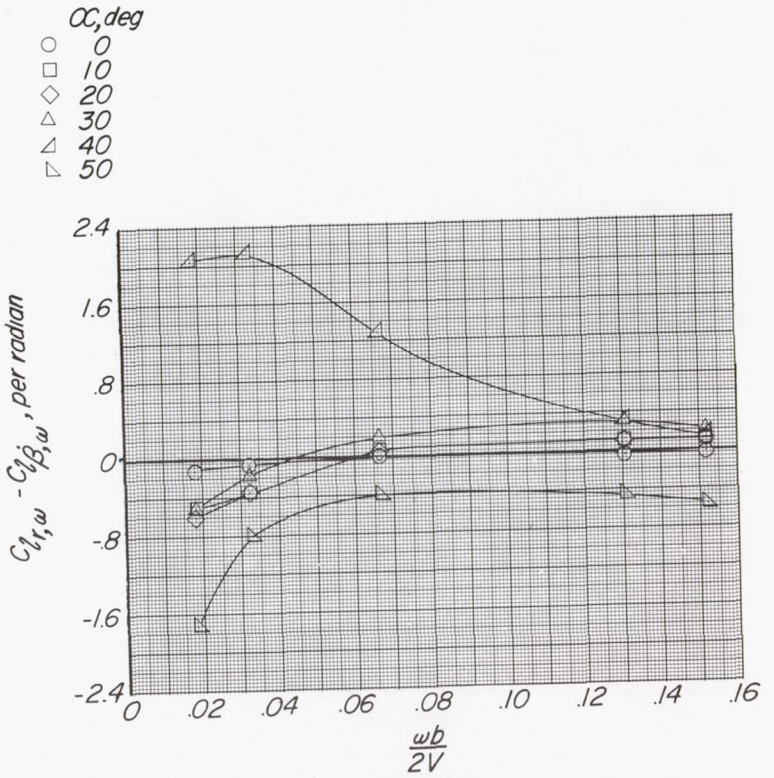

Figure 26.- Variation with frequency parameter of the rolling moment due to yawing parameter for the 75° delta wing. $\psi_o = \pm 6^o$.

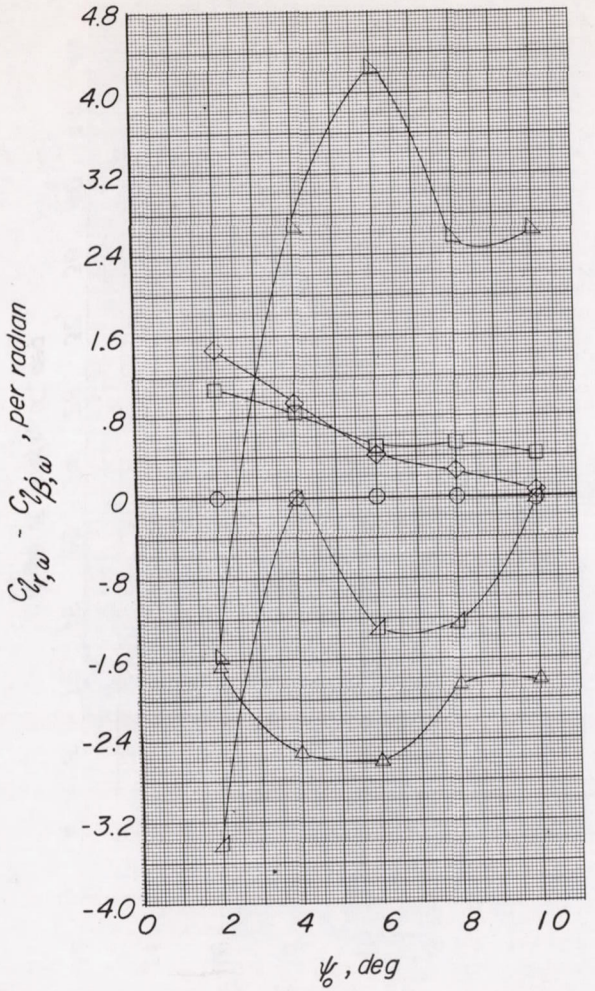

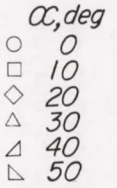

Figure 27.- Variation with amplitude of the rolling moment due to yawing parameter for the 82.5° delta wing. $\omega b/2V = 0.066$.

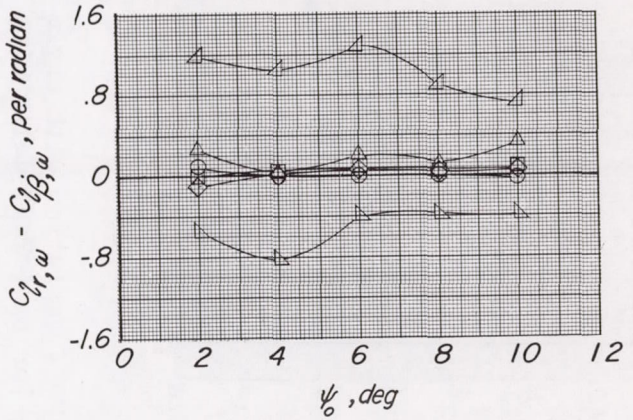

Figure 28.- Variation with amplitude of the rolling moment due to yawing parameter for the 75° delta wing. $\omega b/2V = 0.066$.

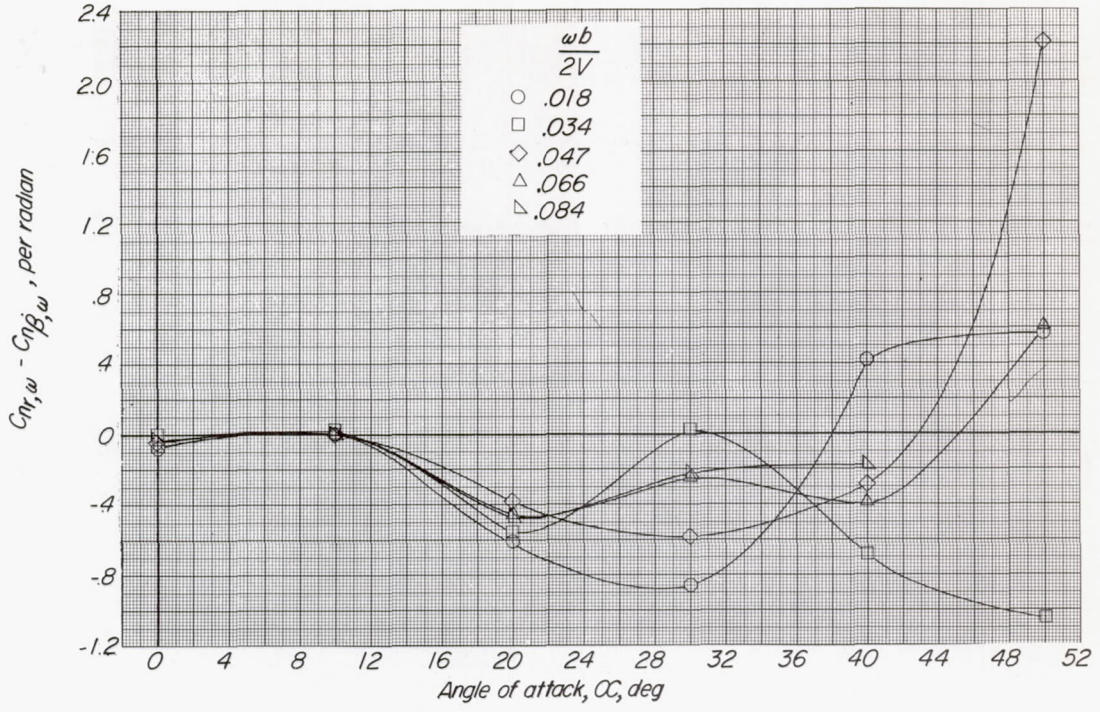

Figure 29.- Variation with angle of attack of the damping-in-yaw parameter for the 82.5° delta wing measured during oscillation. $\psi_o = \pm 6°$.

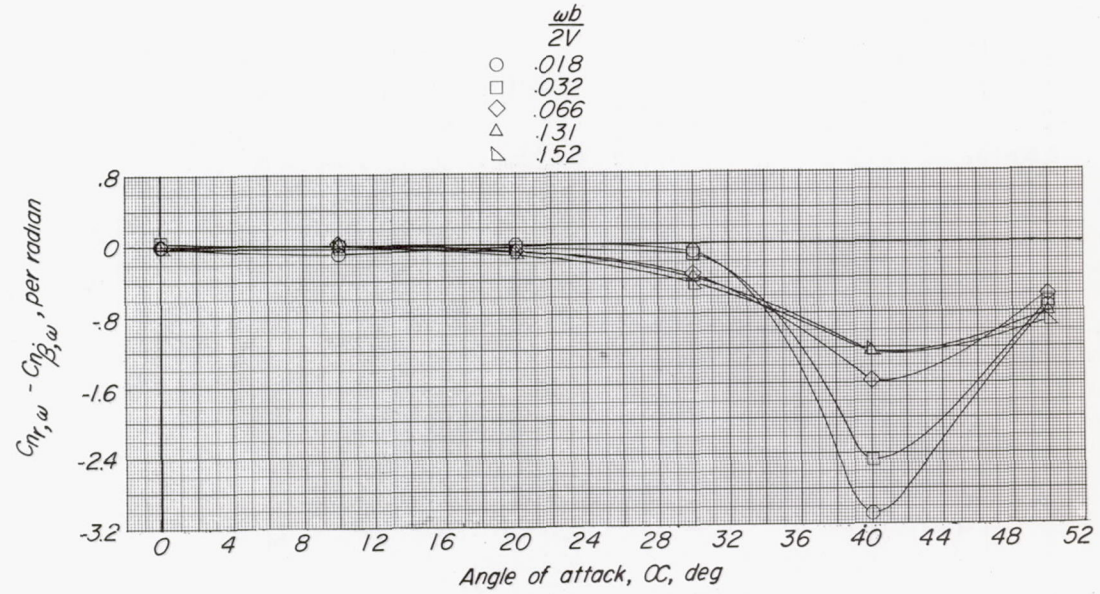

Figure 30.- Variation with angle of attack of the damping-in-yaw parameter for the 75° delta wing measured during oscillation. $\psi_o = \pm 6°$.

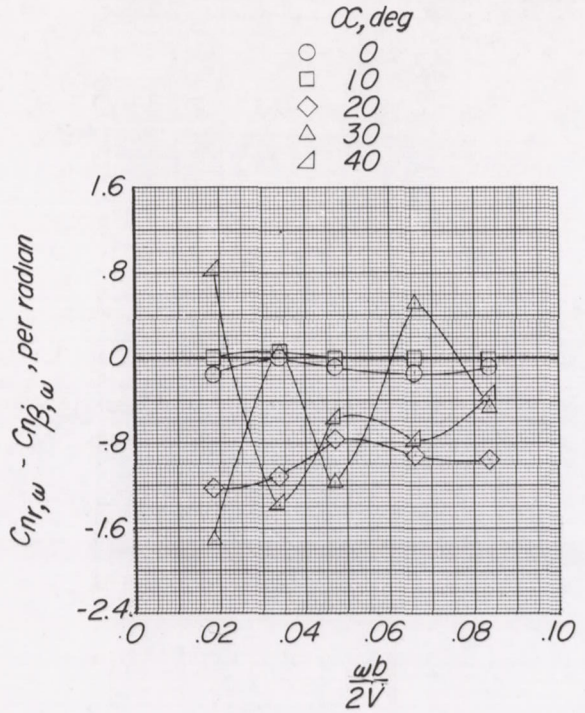

Figure 31.- Variation with frequency parameter of the damping-in-yaw parameter for the 82.5° delta wing. $\psi_o = \pm 6°$.

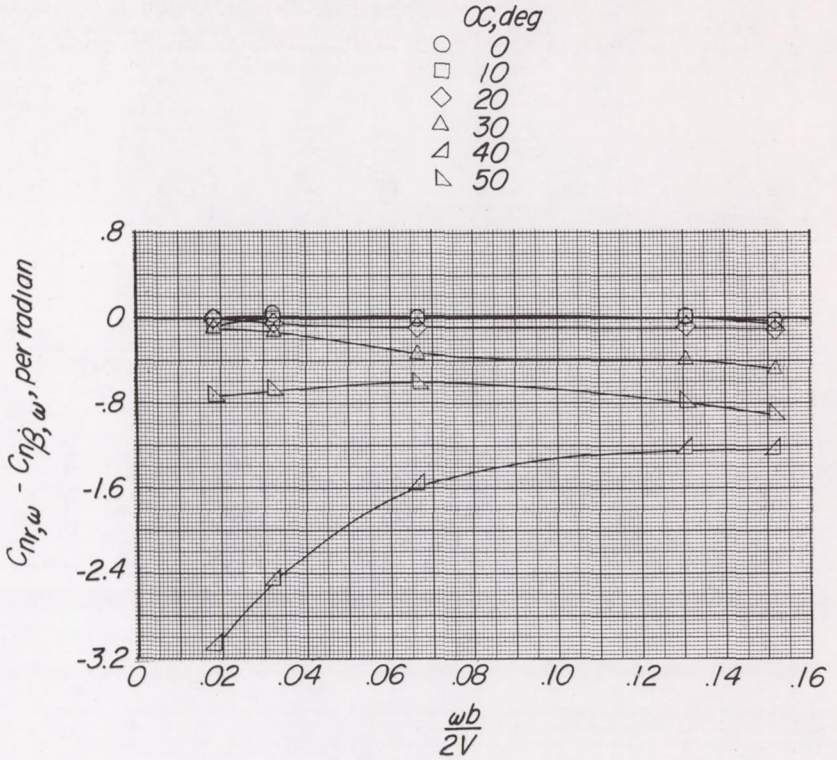

Figure 32.- Variation with frequency parameter of the damping-in-yaw parameter for the 75° delta wing. $\psi_o = \pm 6°$.

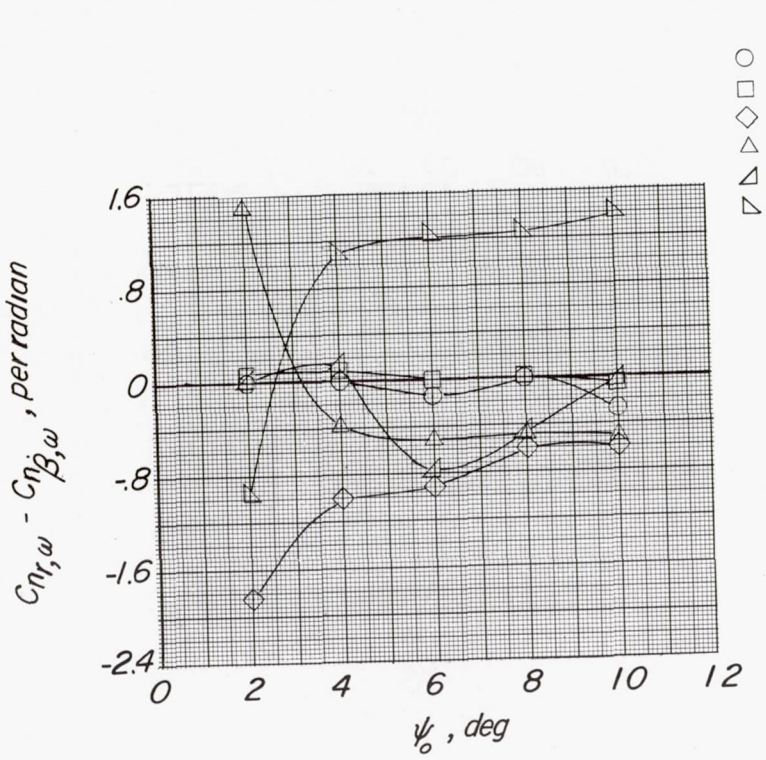

Figure 33.- Variation with amplitude of the damping-in-yaw parameter for the 82.5° delta wing. $\omega b/2V = 0.066$.

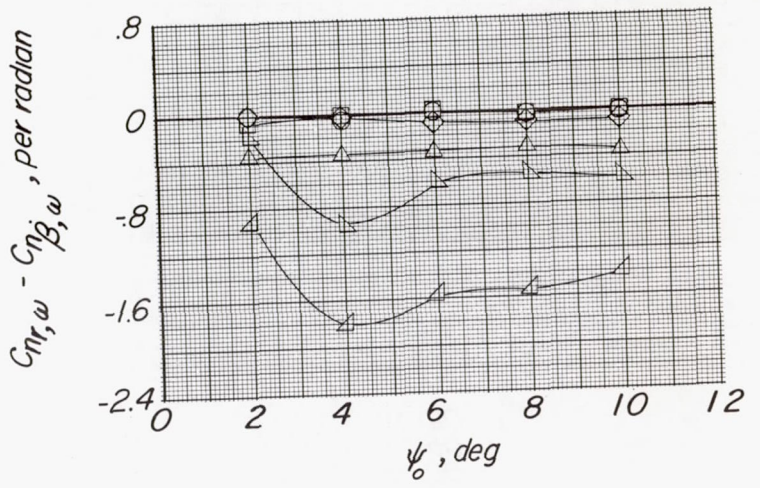

Figure 34.- Variation with amplitude of the damping-in-yaw parameter for the 75° delta wing. $\omega b/2V = 0.066$.

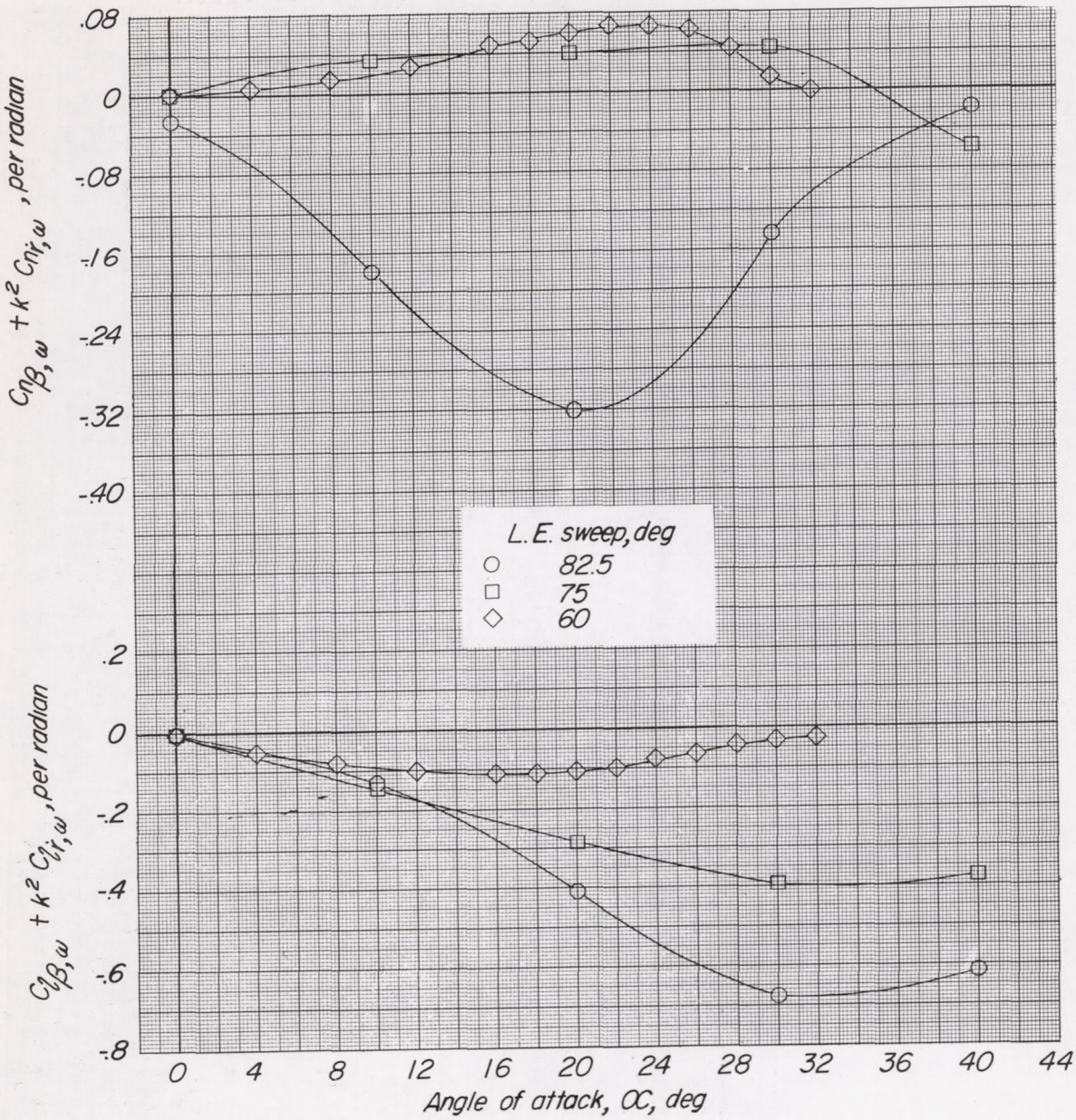

(a) $C_{l_{\beta,\omega}} + k^2 C_{l_{\dot{r},\omega}}$ and $C_{n_{\beta,\omega}} + k^2 C_{n_{\dot{r},\omega}}$.

Figure 35.- Comparison of the variation with angle of attack of the stability derivatives for the 82.5°, 75°, and 60° delta wings measured during oscillation. $\omega b/2V = 0.066$; $\psi_o = \pm 6°$.

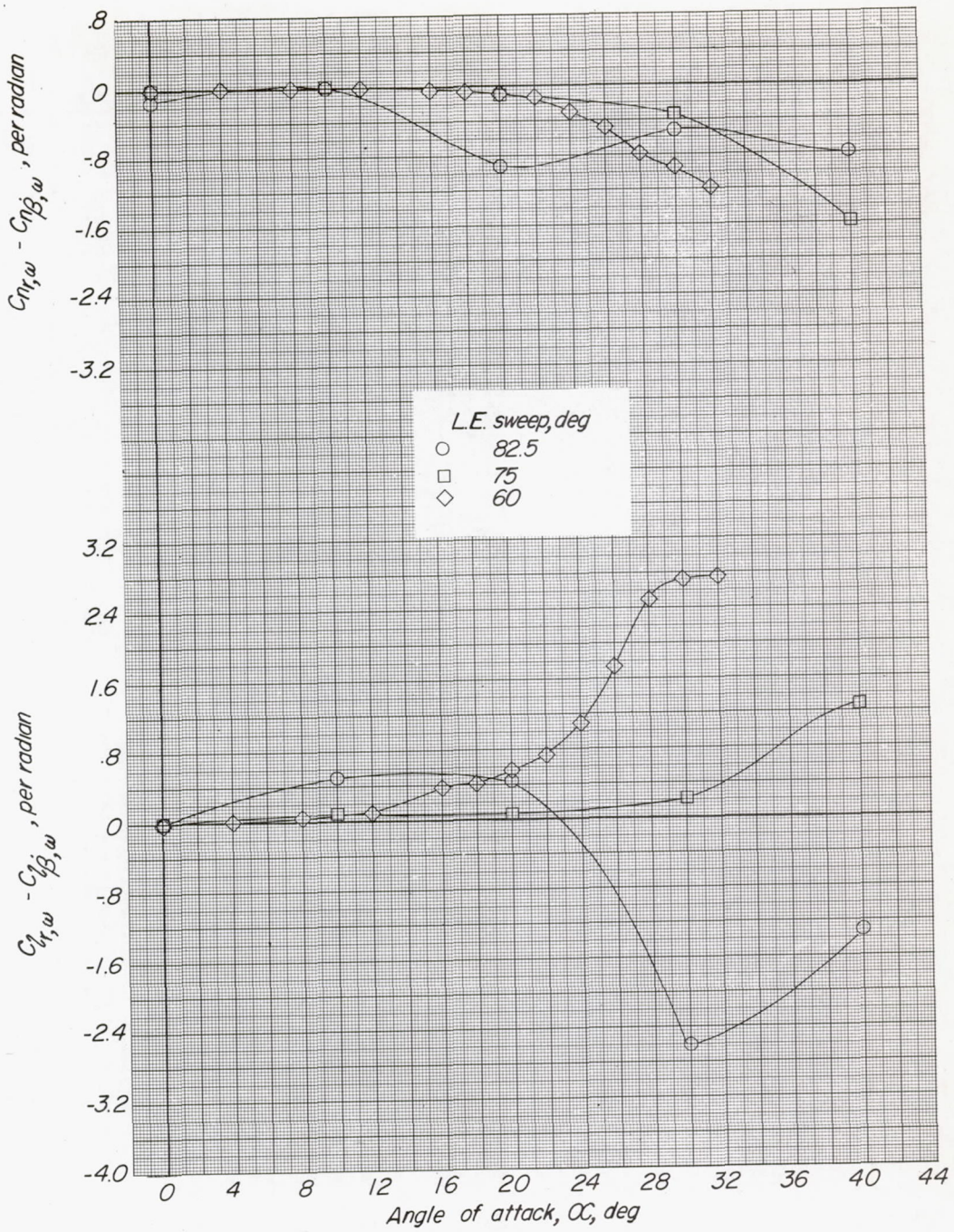

(b) $C_{l_{r,\omega}} - C_{l_{\dot{\beta},\omega}}$ and $C_{n_{r,\omega}} - C_{n_{\dot{\beta},\omega}}$.

Figure 35.- Concluded.